

2015-01-01

# High Performance Computing in Air quality models an their applications

Roberto A. Perea

*University of Texas at El Paso*, raperea@utep.edu

Follow this and additional works at: [https://digitalcommons.utep.edu/open\\_etd](https://digitalcommons.utep.edu/open_etd)



Part of the [Environmental Sciences Commons](#)

---

## Recommended Citation

Perea, Roberto A., "High Performance Computing in Air quality models an their applications" (2015). *Open Access Theses & Dissertations*. 921.

[https://digitalcommons.utep.edu/open\\_etd/921](https://digitalcommons.utep.edu/open_etd/921)

This is brought to you for free and open access by DigitalCommons@UTEP. It has been accepted for inclusion in Open Access Theses & Dissertations by an authorized administrator of DigitalCommons@UTEP. For more information, please contact [lweber@utep.edu](mailto:lweber@utep.edu).

# High Performance Computing in Air Quality Modeling and their Applications

ROBERTO A. PEREA

Environmental Science and Engineering Ph.D. Program

APPROVED:

---

Rosa M. Fitzgerald, Ph.D.

---

William Stockwell, Ph.D.

---

Maria Amaya, Ph.D.

---

Barry Benedict, Ph.D.

---

Russell Chianelli, Ph.D.

---

Charles Ambler, Ph.D.

Dean of Graduate School

Copyright ©

by

Roberto Perea

2015

# High Performance Computing in Air Quality Modeling and their Applications

By

ROBERTO A. PEREA, MSEE

DISSERTATION

Presented to the Faculty of the Graduate School of  
The University of Texas at El Paso  
in Partial Fulfillment  
of the Requirements  
for the Degree of

DOCTOR OF PHILOSOPHY

Environmental Science and Engineering  
THE UNIVERSITY OF TEXAS AT EL PASO

December 2015

## Acknowledgments

First, I would like to acknowledge my dissertation advisor, Dr Rosa Fitzgerald for her guidance and great ideas and the dissertation committee members, Dr Amaya, Dr Benedict, Dr Chianelli and Dr Stockwell for their agreeing and giving advice on my dissertation. Secondly, I would like to acknowledge my mother Virginia Martinez and my sister Alejandra Perea for their moral support and their keep going attitude. Also, I would like to thanks my friends Sergio Zapata, Jaime Orozco and Pablo Adame for their support and unconditional help. Also, I would like to thanks Olga Rodriguez from the Graduate School for her help. Finally, to my father, Alfonso Perea for his support and advise.

## Abstract

High Performance Computing has become an important tool for many applications and services in the areas of Air Quality research. One important aspect is the use of computational technology in simulation and modeling of complex Air Quality models which makes it affordable in terms of data analysis, processing and speed. For this dissertation, three projects using Air quality models were developed using high performance computing.

For the first project, ozone concentrations for the Paso del Norte Region are simulated using air quality models and compared against experimental data. For the second project, the Development of models and optimization of codes to study ozone concentrations in the South Coast Air Basin (Southern California) is presented for emission control strategies. For the third project, the transport of Valley Fever is examined and a model is developed to forecast events of exposure and maximum risk for this region.

## Table of Contents

Acknowledgments.....	iv
Abstract.....	v
Table of Contents.....	vi
List of Figures.....	vii
Chapter 1: Introduction.....	1
Chapter 2: Methodologies.....	21
Chapter 3: Results.....	26
Chapter 4: Conclusion.....	53
References.....	55
Curriculum Vitae .....	59

## List of Figures

Figure 1. Common HPC cluster topology

Figure 2. Air quality model (NOAA)

Figure 3. CAMx Block level diagram

Figure 4. CMAQ Block level model diagram.

Figure 5. WRF Block level diagram

Figure 6. Paso del Norte region

Figure 7. SOCAB area

Figure 8. Valley fever cycle

Figure 9. Endemic areas for Valley fever.

Figure 10. Contour plot of 2008 VOC1.5 - 2008 Base

Figure 11. Contour plot of 2008 VOC2.0 - 2008 Base

Figure 12. Contour plot of 2030 base – 2008 Base

Figure 13. Contour plot of 2030 NO<sub>x</sub> 0.5 – 2008 Base

Figure 14. Contour plot of 2030VOC1.5NO<sub>x</sub>0.75 - 2008 Base

Figure 15. Contour plot of 2030NO<sub>x</sub>0.3 - 2008 Base

Figure 16. Contour plot of 2030VOC1.5NO<sub>x</sub>0.5 - 2008 Base

Figure 17. Contour plot of 2030VOC1.5NO<sub>x</sub>0.75 - 2008 Base

Figure 18. Contour plot of 2030VOC1.5NO<sub>x</sub>0.3 - 2008 Base

Figure 19. Contour plot of 2030VOC1.5NO<sub>x</sub>1.0 - 2008 Base

Figure 20. Hysplit result of the dust event

Figure 21. Windrose result of the Dust event

Figure 22. Satellite image of the dust storm.



Figure 23. Contour plot of PM 10

Figure 24. Contour plot of PM 2.5

## List of Graphs

Graph 1. Valley fever incidence in 2012

Graph 2. Results from station 6ZK

Graph 3. Results from station 6ZN

Graph 4. CMAQ vs Observed simulation for base 2008.

Graph 5. CMAQ simulations with factors of 1.5 and 2.0 VOC against 2008 base and observed values.

Graph 6. CMAQ (Continued) simulations with factors of 1.5 and 2.0 VOC against 2008 base and observed values.

Graph 7. CMAQ simulations with factors of 0.75, 0.50 and 0.30 NO<sub>x</sub> against 2030 base.

Graph 8. CMAQ (Continued) simulations with factors of 0.75, 0.50 and 0.30 NO<sub>x</sub> against 2030 base.

Graph 9. CMAQ simulations with factors of 0.75, 0.50 and 0.30 NO<sub>x</sub> against 2030 base with 1.5 of VOC.

Graph 10. CMAQ (Continued) simulations with factors of 0.75, 0.50 and 0.30 NO<sub>x</sub> against 2030 1.5 VOC.

Graph 11. Weather conditions at Azcarate Monitoring station

Graph 12. Sounding chart from the University of Wyoming

Graph 13. WRF PBLH result for April 14, 2012

# Chapter 1

## Introduction

High Performance Computing has become an important tool for many applications and services in the areas of Air Quality research. One important aspect is the use of computational technology in simulation and modeling of complex Air Quality models which makes it affordable in terms of data analysis, processing and speed. For this dissertation, three projects were developed using high performance computing.

For the first project, ozone concentrations for the Paso del Norte Region are simulated using air quality models and compared against experimental data. For the second project, the Development of models and optimization of codes to study ozone concentrations in the South Coast Air Basin (Southern California) is proposed for emission control strategies. For the third project, the transport of Valley Fever is examined and a model is developed to forecast events of exposure and maximum risk for this region.

An overview of the high performance computing resides in the use of a master computer node and several slave computer nodes connected by a high speed local area network. In general, a grouping of several computer is called a cluster, which provides high availability (if one nodes goes down the system continue to function) and higher processing power (multiple nodes processing information as a group instead of one node individually). Usually the network topology is a stackable set of switches on n-node ring (Amit Jain). This allows several switches to be connected in a stack and all the nodes can interact between each other without having a barrier.

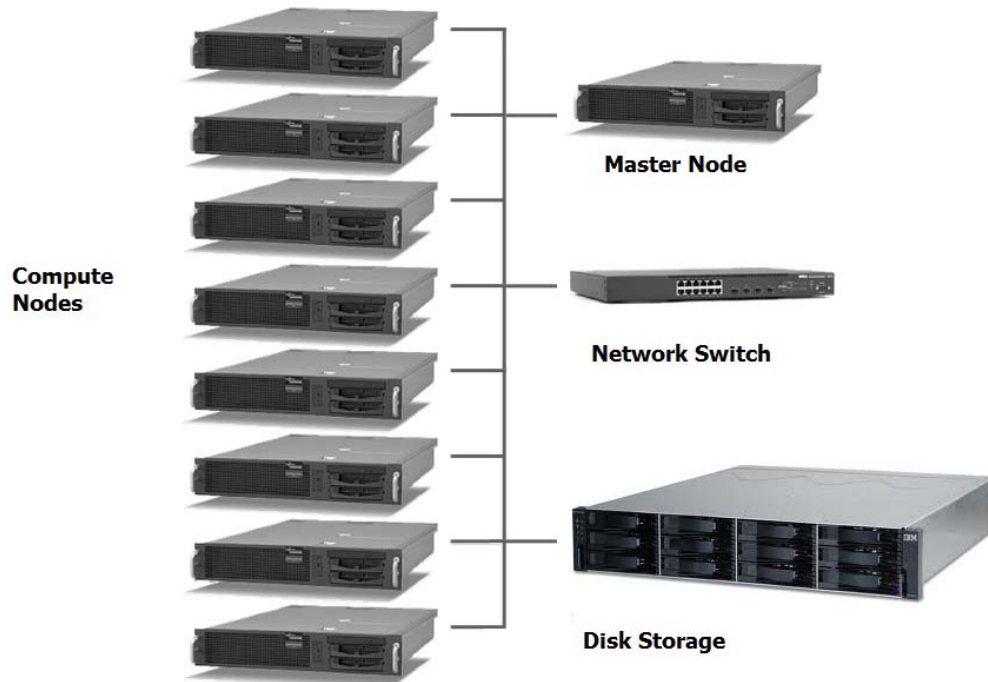


Figure 1. Common HPC cluster topology

A scheduler/resource manager is a software sub-system that monitors and receives job (data simulation) requests from the user, set the queues for the jobs and then submits for processing into the nodes. For example, if a job is submitted through the master node, the scheduler will check if there are resources available at the moment, if not the job goes to a queue mode and waits until resources became free. Once, there is availability, the job is ready for processing (Abhishek Gupta).

The message parsing interface is a library interface, which serves to move data from one process to another. This is useful to manage memory and avoid waste of resources by sharing set of memory between processes (W. Gropp, E. Lusk, and A. Skjellum).

The parallel virtual machine is a software package that permits a heterogeneous collection of computers clustered together by a network to be used as a single large parallel computer.

Therefore, large computational data can be processed faster by using the aggregate power and memory of many computers (V. S. Sunderam).

All subsystems in combination, creates a functional High performance computing system. The additional feature in the infrastructure is the data storing and easy access for the users, which is based on a web based open source sharing file system. This system in conjunction with the storage and backup solution will provide a reliable central point for archiving data.

Air quality models use a series of equations to simulate the physical and chemical processes that affect air pollutants as they disperse and react in the atmosphere in a certain geographical area. Based on inputs of meteorological data and chemical source information, these models are designed to characterize primary pollutants that are emitted directly into the atmosphere and, in some cases, secondary pollutants that are formed because of complex chemical reactions within the atmosphere. These models are important to the air quality system because of the management and control of air pollution and to identify both source contributions to air quality problems and assist in the design of effective strategies to reduce harmful air pollutants. Air pollution comes from many different sources: stationary sources such as factories, power plants, and smelters; mobile sources such as cars, buses, planes, trucks, and trains. For example, air quality models can be used during the permitting process to verify that a new source will not exceed ambient air quality standards or, if necessary, determine appropriate additional control requirements. In addition, air quality models can also be used to predict future pollutant concentrations from multiple sources after the implementation of a new regulatory program, in order to estimate the effectiveness of the program in reducing harmful exposures to humans and the environment. An Air quality model requires the chemical sources in a form of datasets, mostly coming from stations, geographical data of the area such as the coordinates for the

domain, terrain characteristics and meteorological or physical elements like wind speed, diffusion, dispersion, albedo, mechanism of transport for mass (flow) and energy (advection).

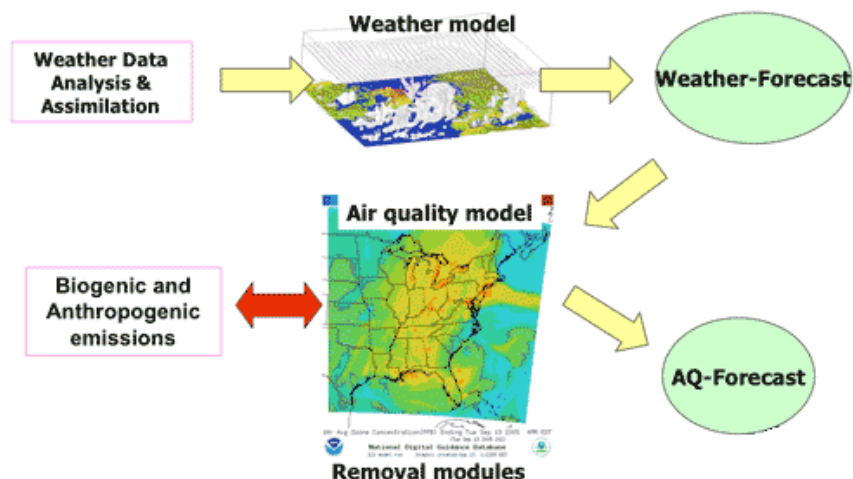


Figure 2. Air quality model (NOAA)

The two most used programs for air quality modeling are Comprehensive Air quality with extensions (CAMx) and Community Multiscale Air Quality (CMAQ). CAMx is an Eulerian photochemical dispersion model that allows for integrated "one-atmosphere" assessments of gaseous and particulate air pollution (ozone, particulate matter, air toxics) over spatial scales ranging from neighborhoods to continents. It uses parallel processing using Open-MP on shared-memory systems and Parallel processing using Message Passing Interface (MPI) on distributed-memory systems. CAMx can use input fields from meteorological models (WRF, MM5) and emission inputs (SMOKE, EPS3, EMS, SAPRC) and Multiple gas phase chemistry mechanism options (CB6, CB05).

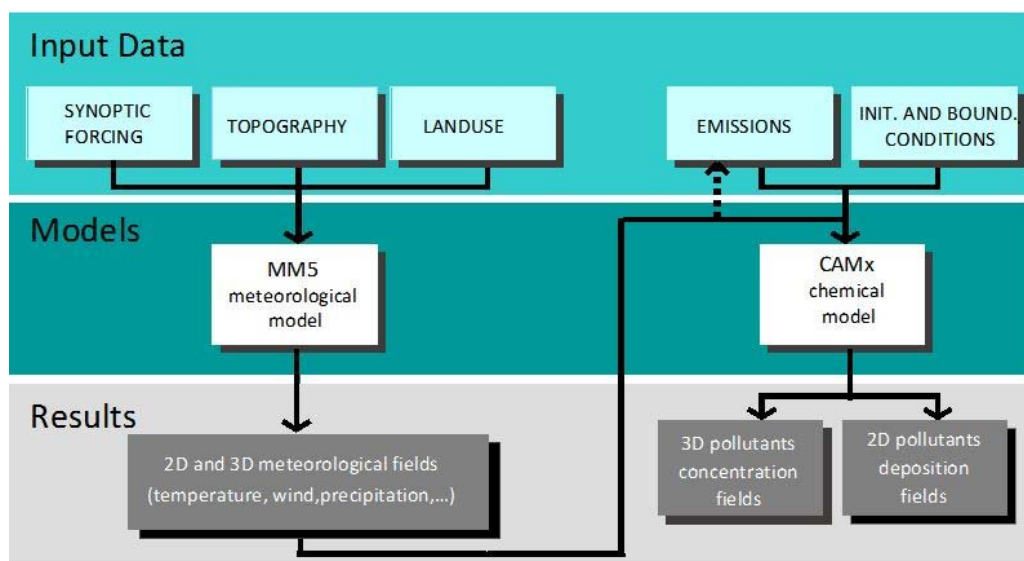


Figure 3. CAMx Block level diagram

CMAQ uses an Eulerian model coupled with ordinary differential equations to predict pollutant concentrations in a 3D grid. Also, it uses Carbon bond 5 which is a mechanism of atmospheric oxidant chemistry that provides modeling of ozone, particulate matter, visibility, acid deposition and others. It has support for MPI on distributed computing. The following processes are used, Emissions from sources, horizontal and vertical advection, horizontal and vertical diffusion, chemical transformations and Loss processes (deposition).

Atmospheric aerosol particles are referred to as particulate matter (PM) and can be either primary or secondary. Primary PM is emitted directly into the atmosphere from natural or anthropogenic sources. Secondary PM is formed in the atmosphere, either from precursors that react chemically to form new particles, or from vapor phase species that condense or deposit onto primary particles that are already present in the atmosphere or cloud processes. Atmospheric particulate matter (PM) is linked with acute and chronic health effects, visibility degradation, acid and nutrient deposition, and climate change. Accurate predictions of the PM mass concentration, composition, and size distribution are necessary for assessing the potential

impacts of future air quality regulations and future climate on these health and environmental outcomes (EPA, Atmospheric Modeling and analysis Research). The two-way coupling of WRF (Weather Research Forecasting) and CMAQ enables interaction between aerosols and meteorology. In Community Multiscale Air Quality (CMAQ) model, aerosol information is used for optical properties in WRF's radiation calculations thus enabling an examination of the direct effect of aerosols.

CMAQ Chemistry Transport Model (CCTM) represents PM using three lognormal sub distributions, or modes. Two interacting modes (Aitken and accumulation) represent PM<sub>2.5</sub> (particulate matter of diameter equal to or less than 2.5 microns). A coarse mode represents PM with diameters greater than 2.5 microns and equal to or less than 10 microns. Thus, PM<sub>10</sub> is modeled as the sum of the PM<sub>2.5</sub> and coarse-mode PM. Particulate matter is deposited to the ground by wet or dry deposition, both of which are modeled by CMAQ. In wet deposition, PM is transferred by rainfall. Wet deposition is calculated within CMAQ's cloud module.

In dry deposition, the transfer is by turbulent air motion and by direct gravitational sedimentation of larger particles. The deposition velocity for particles must be calculated from the aerosol size distribution and from meteorological and land-use information. CMAQ's dry deposition module calculates the size distribution from the mass and number concentration for each of the three modes and then calculates the dry deposition velocity. In CMAQ, several new pathways for secondary organic aerosol (SOA) formation have been implemented, based on the recommendations of Edney et al. (2007) and the recent work of Carlton et al. (2008). New SOA precursors include isoprene, sesquiterpenes, benzene, glyoxal, and methylglyoxal. The enthalpies of vaporization of these species have been revised based on recent laboratory data (Edney et al., 2007). In previous versions of CMAQ, all SOA was treated as semivolatile. In CMAQ, four



types of nonvolatile SOA are simulated. There is a new surface interaction module in the multipollutant version of CMAQ that calculates the flux of mercury to and from the surface (rather than just depositing mercury). Another type of output available from CMAQ is the reduction in visual range caused by the presence of PM, perceived as haze. CCTM integrates Mie scattering (a generalized particulate light-scattering mechanism that follows from the laws of electromagnetism applied to particulate matter) over the entire range of particle sizes to obtain a single visibility value for each model grid cell at each time step. For easier comparison of CMAQ's output PM values with measurements, there are three new variables (PM25AT, PM25AC, and PM25CO) that are the fractional amounts of the Aitken, accumulation, and coarse modes, respectively, that are composed of particles less than 2.5 microns in aerodynamic diameter (Jiang et al., 2006).

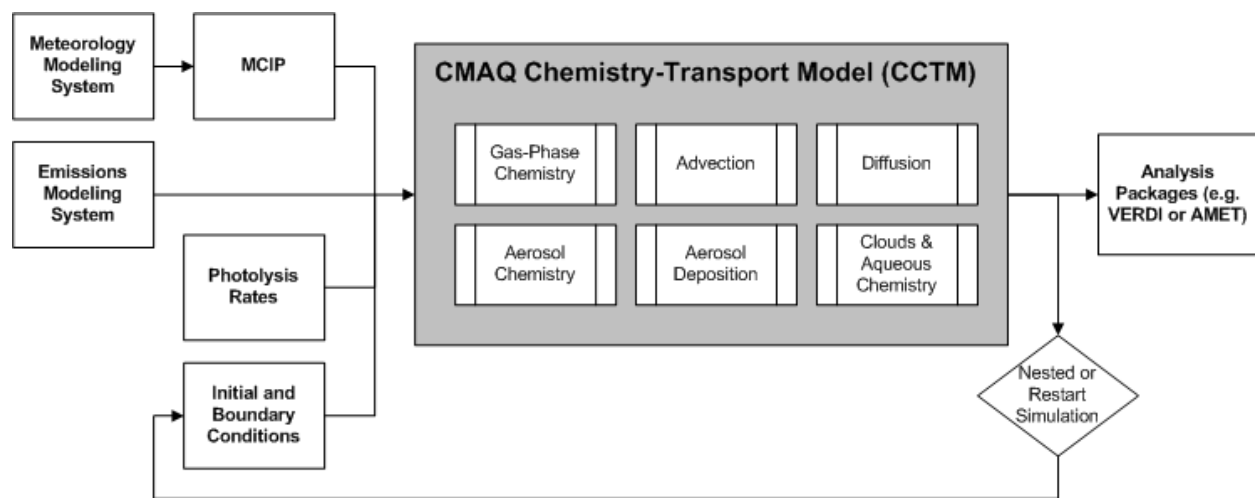


Figure 4. CMAQ Block level model diagram.

The meteorological factor involved in the transport and mechanism of the weather dynamics includes:

The term advection is the transport of energy, mass and momentum from one area to another, in this case temperature, humidity and chemical compounds using wind flows as a medium of movement. The geostrophic flow is defined as the movement in parallel to the height contour. The horizontal component of the Coriolis force and pressure gradient force are in balance. The cyclostrophic flow is defined as the Coriolis force being neglected and the pressure gradient and centrifugal force are in equilibrium. (Holton, James R)

The mechanism of transport of chemicals in the atmosphere by random movements occurs by diffusion and dispersion. In diffusion, the movement of molecules occurs due to kinetic energy, leading to a spread out. Usually, this movement is associated with turbulent flows, but slower and in lower scalar. However, dispersion moves more rapidly and in a larger scale. Diffusion moves compounds from areas of high concentration to areas of low concentration with respect on time.

For the transports of masses on the atmosphere using wind, the flow mechanism is included. The types of flows involved on the boundary layer are important to the transport, diffusion and dispersion of chemical compounds. The following are the most predominant types of flows in the meteorological aspect. Turbulent flows contain irregular quasi-random motions or eddies which cause air areas to drift apart and mix properties such as momentum and temperature across the boundary layer. The boundary layer is defined as a separation of two areas, one inside where viscosity and drag is a part of the variables and the outside where those conditions are neglected. In the inside layer, these maintain a transport of heat and humidity away from the surface while keeping a conservation of momentum. The measurement is occurs on Reynolds numbers or non-dimensional velocity defined by the ratio of pressure and stress. At high Reynolds numbers,

turbulent flows occurs while at low ratio laminar flow is predominant, is more stable, and parallel (Seinfeld, J. and S. Pandis).

The planetary scattering albedo is a function of the optical properties of objects within the atmosphere (e.g., clouds, water vapor, and aerosols) and objects that constitute the planet's surface (e.g., ice, ocean, and trees). It is convenient to lump the atmosphere's contribution to planetary albedo into three bulk processes: clouds and aerosols that directly reflect incident solar radiation back to space, atmospheric opacity to down welling shortwave radiation that limits the amount of down welling shortwave radiation reaching the surface and atmospheric opacity to shortwave radiation. Surface reflection accounts for less than 25% of the climatological planetary albedo in the ice- and snow-covered regions of the planet and the remainder is due to clouds (Donohoe, Aaron S, A.Venkatram, and Battisti, David).

The coordinates used can be fixed at one point or Eulerian or following the flow, called lagrangian. The latter, uses the coordinate system for particles or molecules that follow a wind vector and speed.

Wet deposition occurs when there is a precipitation like rain, snow is present and the material is settled down on the surface. Otherwise, dry deposition occurs when the material falls down by means of gravity.

In order for an Air quality model to work, it needs meteorological data from a simulation. The Weather Research and Forecasting (WRF) Model is a next-generation mesoscale numerical weather prediction system designed to serve both atmospheric research and operational forecasting needs WRF allows researchers to generate atmospheric simulations based on real data (observations, analyses) or idealized conditions. WRF offers operational forecasting a

flexible and computationally-efficient platform, while providing advances in physics, numeric, and data assimilation contributed by developers in the broader research community. It features two dynamical cores, a data assimilation system, and a software architecture facilitating parallel computation and system extensibility.

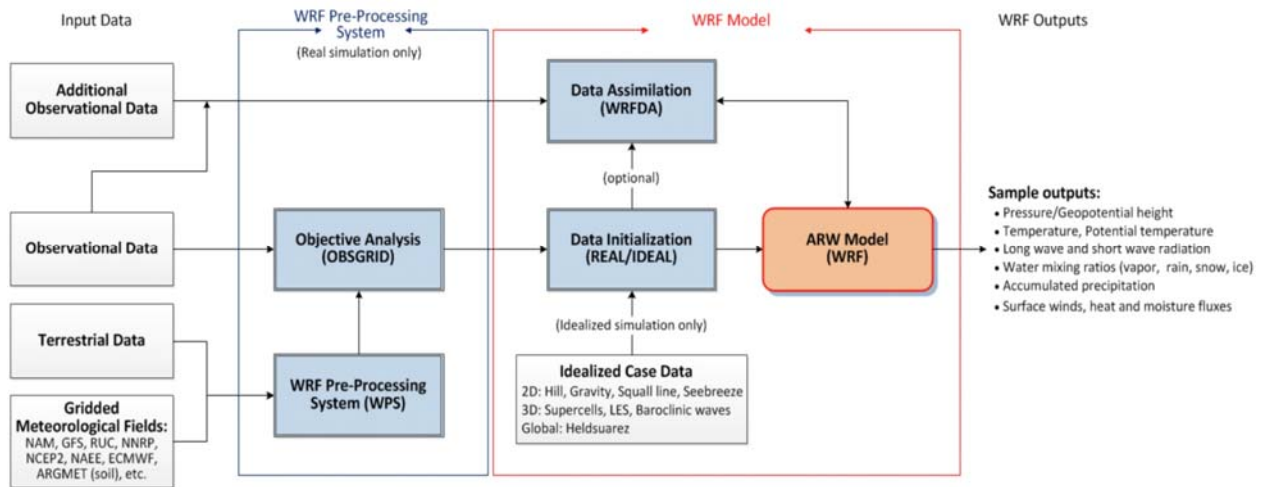


Figure 5. WRF Block level diagram

The geographical area contains a domain, which contains smaller sub-divisions called cells in a sectioned grid. The grid is divided by its vertical and horizontal properties and most models use Cartesian or polar system. Regular Cartesian grids are specified by the Start and Finish X, Y and Z coordinates, representing the minimum and maximum values in each direction, together with the Number of points along the X, Y and Z axes. Regular polar grids are specified by the location of the origin of the polar grid (X and Y coordinates), plus the Start and Finish values of the radius, the angle and the heights, together with the number of points in the radial direction, the number of angles into which the circumference is divided and the number of heights.

Another part is the domain grid, which offers the levels of resolution and projection of the simulation on a terrain plane. The grid staggering is the Arakawa C-grid. The model uses the

Runge-Kutta 2nd and 3rd order time integration schemes and 2nd to 6th order advection schemes in both horizontal and vertical directions. It uses a time-split small step for acoustic and gravity-wave modes.

For the first project, the objective was to study the difference of ozone simulations made by three-dimensional atmospheric chemical models in The Paso del Norte region. Ozone concentration in the atmosphere is the major contribution to earth oxidizing capacity (Thompson) and at the local level or tropospheric level is a high threat to human health (Lu et al, Stockwell et al). Regional and Global atmospheric chemistry models are used to estimate the emissions and its effects on oxidizing capacity and to develop strategies for air pollution control on regional and local levels. On these models an important element is the chemical mechanism, which is a list of reactions and equations that describes the chemical transformations of emissions, acid deposition and aerosols that lead to ozone formation. The chemical mechanism used for most computer models are the carbon bond model 4 and 5 (CB4, CB5; Gery et al; Yarwood et al,) and the Statewide Air Pollution Research Center mechanism (SAPRC, Carter). These mechanisms are constantly updated and revised for modeling urban and regional conditions, but their conceptual formulation remains more focused to more polluted conditions. Therefore, many of the evaluations examine performance of air quality mechanism for high concentrations but not for low concentrations.

The chemical mechanism are evaluated by comparing simulations against environmental chamber data where the effects of meteorology are absent; inter comparison of chemical mechanism using 1-D chemistry models (Olson et al) and comparison of 3-D air quality models (Byub et al). Studies made with more advanced instrumentation are often performed during episodes of high ozone pollution. However, typical atmospheric conditions are studied through

routine measurement networks. The result is that air quality mechanisms and air quality models are not well observed or evaluated at lower concentration that they forecast and yield the possibility of bias in the creation of mechanism.

A more serious problem in the air quality models is that they underestimate the response of ozone to changes in emissions and meteorology (Gilliland et al) found much less variability in their modeled ozone in comparison with measurements.

The Comprehensive Air Quality Model with Extensions (CAMX; Environ) was used to make simulations with the CB4 and CB5 mechanisms. The Paso del Norte region forms the largest contiguous bi-national conglomerate on the US-Mexico border. The air pollution meteorology of the region is typical of the Western United States. The predominant synoptic feature of an episode of high ozone in the Paso del Norte region is the expansion, intensification, and slow progression of an upper-level ridge of high pressure.

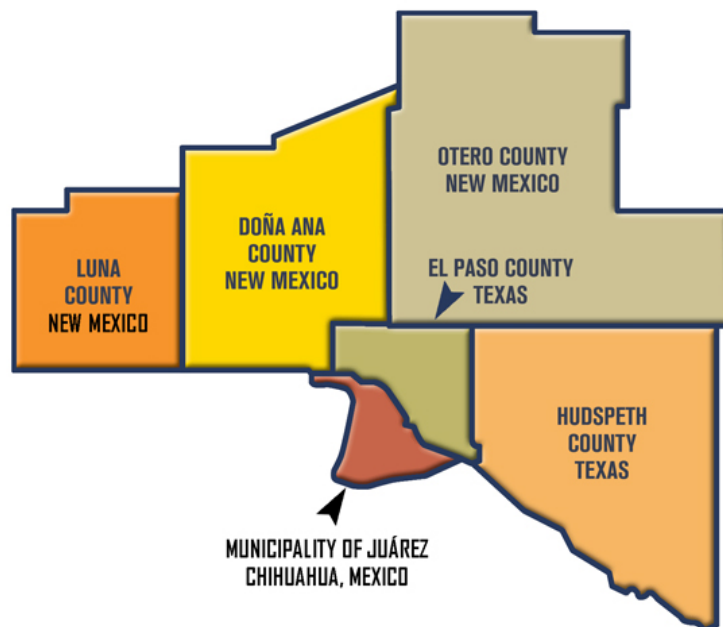


Figure 6. Paso del Norte region

This region is located at the intersection of two countries and three states, and is comprised of the American cities of El Paso, Texas and Sunland Park, New Mexico; as well as the Mexican city of Ciudad Juarez, Chihuahua. With a combined population of around 2 million inhabitants, the Paso del Norte region is isolated, more than 500 km away from the nearest urban area of comparable size, thus making it an ideal location for air quality studies of an isolated urban environment. The meteorology of this area is associated with a highly stable atmosphere, strong temperature inversions with low mixing heights and therefore low mixing volumes. Under these conditions emissions lead to highly polluted conditions that are favorable to ozone formation. The Paso del Norte region was used as a test-bed for these simulations because of its location and our previous experience with the modeling of this region (Lu et al).

For the second project, a study examined the effects of varying reductions in emissions of NO<sub>x</sub> and Volatile organic compounds in the California's South Coast Air Basin (SoCAB), where has historically experienced the most severe ground-level ozone (O<sub>3</sub>) pollution in the United States. The basin is 10,743 square miles and has a population of over 17.8 million people (2010 U.S. Census). Four decades of progressively more stringent controls of volatile organic compound (VOC) and oxides of nitrogen (NO<sub>x</sub>) emissions have reduced the number of exceedances of the 2008 eight-hour ozone National Ambient Air Quality Standard (NAAQS). Prior to the implementation of emission reduction measures in the early 1950s, hourly averaged ozone mixing ratios at alarming concentrations were relatively frequent events in the 1960s. However, the current ozone NAAQS is exceeded in the basin on most summer days and to achieve the standard by the 2032 deadline remains a long-term challenge. High mountains, adverse meteorology that results in low mixing layers and conditions that limit atmospheric dispersion and emissions from adjacent counties within the semi-permanent high-pressure zone of the eastern Pacific lead to high concentrations of ozone. Frequent temperature inversions are caused by descending air that warms when it is compressed over cool, moist marine air. These inversions often occur during periods of maximum solar radiation. On-shore breeze is strong during the day and winds are calm overnight with a weak land-sea breeze, flow patterns are from the west and south during the morning, switching to west winds by the afternoon. Heating of the Mountains during the daytime causes up flows that can transport pollutants from the surface into the upper parts, when the slopes cool after sunset, the denser air flows back into the basin with pollutants entrained in it.

Reductions of VOC and NO<sub>x</sub> can have varying effect on the rate and efficiency of ozone formations. Lowering NO<sub>x</sub> effectively reduces Ozone while reductions in VOC have practically



no effect. Ozone is reduced near the ridgeline by simultaneous reductions in VOC and NO<sub>x</sub> emissions. In the “VOC-limited” or “VOC-sensitive” region above the ridgeline, lowering VOC effectively reduces O<sub>3</sub>. However, NO<sub>x</sub> reductions can increase O<sub>3</sub> under VOC-limited conditions by lowering the rate at which OH and NO<sub>2</sub> are removed by formation of HNO<sub>3</sub>. “NO<sub>x</sub>-disbenefit” refers to this situation. NO<sub>x</sub> disbenefit, though counterintuitive, is a well-established aspect of ozone photochemistry and is rooted in the nonlinear nature of the ozone-precursor relationship. The evolution of the ozone-precursor relationship in the SoCAB during the past four decades reflects the corresponding changes in VOC and NO<sub>x</sub> emissions. Control of either NO<sub>x</sub> or VOC alone or simultaneous control of both precursors would have been effective at the time. However, emission control technology development allowed for earlier and more effective control of VOC and CO than NO<sub>x</sub>.

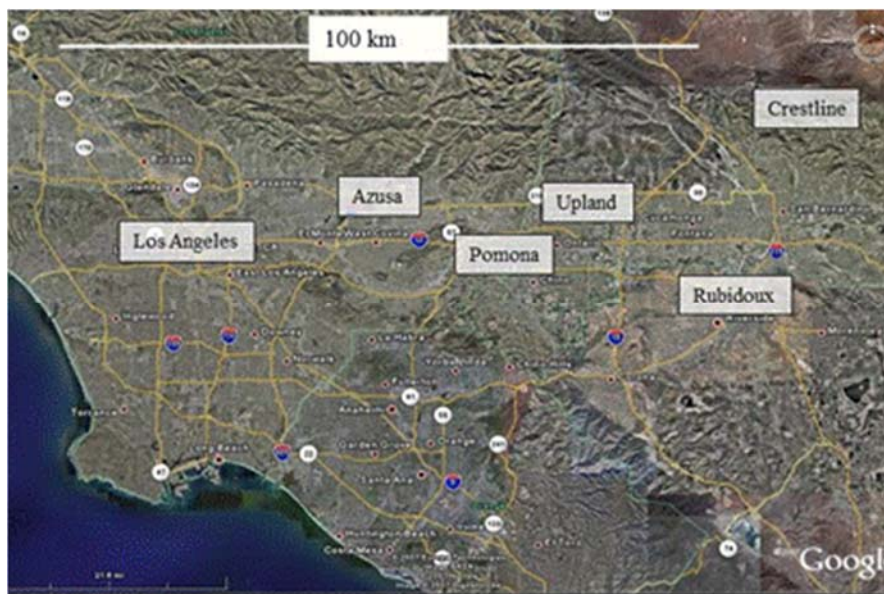


Figure 7. SOCAB area

Ambient VOC/NO<sub>x</sub> ratios initially reflect the mix and type of local emission sources, but increase with time during atmospheric transport of emissions because the HO radical reacts more rapidly with NO<sub>2</sub> than VOC. This causes ambient NO<sub>x</sub> mixing ratios to decrease during the day relative to VOC leading to varying, but generally higher, VOC/NO<sub>x</sub> ratios, while NO<sub>x</sub> reductions can be counter-productive under VOC-limited conditions in and near the source areas (e.g. western and central SoCAB), they can ultimately lead to lower peak ozone levels in downwind receptor locations (e.g. eastern SoCAB). Substantial NO<sub>x</sub> reductions would be required to eliminate NO<sub>x</sub> disbenefit and fully transition ozone formation from VOC to NO<sub>x</sub> limitation in the source areas. In contrast, VOC reductions alone effectively reduce ozone within and near-downwind areas, but are less effective for far-downwind receptor locations and with concurrent NO<sub>x</sub> reductions. The results predicted a period of NO<sub>x</sub> disbenefit for the SoCAB between 2010 and 2020 with planned emission reductions of 50 percent for NO<sub>x</sub> and 10 percent for VOC. Ozone formation was predicted to become precursor limited by 2020 with greater NO<sub>x</sub> reductions of 75 percent, but with higher initial ozone formation rates than in 2005. Peak ozone formation rates in 2020 were predicted to increase on weekdays by a factor of three relative to 2005 and be comparable to ozone rates on weekdays in 1995 and Sundays in 2005 (Fujita et al., 2013). While these future changes would likely result in lower ozone levels in downwind areas where transport is more important than local production of ozone, the location of peak ozone levels were predicted to shift westward toward the central basin. The weekday VOC/NO<sub>x</sub> ratios have increased during the past decade to about 5 to 6 and are projected to increase with greater future emphasis on NO<sub>x</sub> controls. While ozone levels have continue to decline slowly during the past decade at downwind locations (e.g., current basin design value site at Crestline in the San Bernardino Mountains), the weekday ozone trends in the central basin have flattened and even

increased at some central basin locations (Fujita et al). This study focused on the effects of varying reductions of NO<sub>x</sub> and VOC emissions on the location and magnitude of peak ozone levels within the basin, and the persistence and magnitude of an interim period of elevated ozone levels that could result from a NO<sub>x</sub>-focused control strategy in some areas of the SoCAB prior to transition from VOC-sensitive to NO<sub>x</sub>-sensitive ozone formation. It also examined the implications of underestimating current inventories of VOC emissions as well as shortfalls in the prescribed levels of NO<sub>x</sub> emission reductions by forecasting the response of ozone to varying reductions in NO<sub>x</sub> emissions with alternative base VOC emissions.

For the third project, studies on the meteorological conditions that lead to valley fever or Coccidioidomycosis were conducted. Valley fever is an endemic disease from the Southwest (California, Arizona, New Mexico, Texas and North Mexico), where is caused by inhalation of the fungi *Coccidioides posadissi* and *Coccidioides immitis*. The fungi cause an infection with pneumonia or influenza like symptoms and can be lethal if not treated. The disease can progress to chronic or progressive lung disease. They develop into pods that are filled with even tinier seeds. The pods burst open; the seeds pour out and spread in the lung and sometimes to other parts of the body. Wherever the spores settle down, the body reacts with inflammation. In the lungs, little patches of inflammation develop around the spores. Cavities or scars may result, and eventually deposits of calcium. When the spores stay in the lungs, the disease is said to be in its primary form. When the fungus spreads throughout the body, internal organs, bones, brain, and skin is in its disseminated form. Progressive pulmonary coccidioidomycosis includes the above symptoms but progresses to lung volume loss, fibrosis and inflammation, considered serious complications of the disease.

## Biology of Coccidioidomycosis

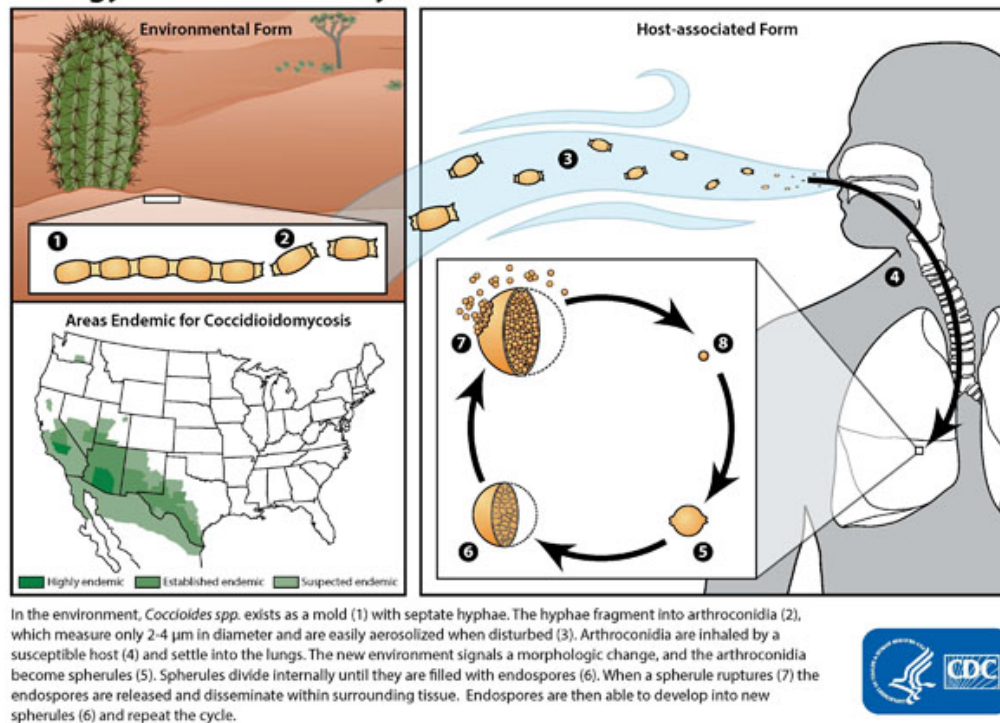


Figure 8. Valley fever cycle

Interest in coccidioidomycosis has been renewed because of massive migration to the Sunbelt states. Areas that were once sparsely populated are now major cities, which increase the population at risk for the disease, like Phoenix and Tucson, Arizona; Bakersfield and Fresno, California; and El Paso, Texas. Interest also has increased because of an explosion in the number of cases that occurred during the great coccidioidomycosis outbreak in California in 1991-1994. The area of study is Arizona as a source and Paso del Norte region as destination for the deposition. In order to study the favorable conditions for the transport and dispersion of the valley fever, several meteorological variables must be met. High winds from the west coming from the Arizona area with sustained speeds of 30 miles per hour and gust of over 50 mph, low humidity (10% or below), low pressure and a disturbance such a dust storm.

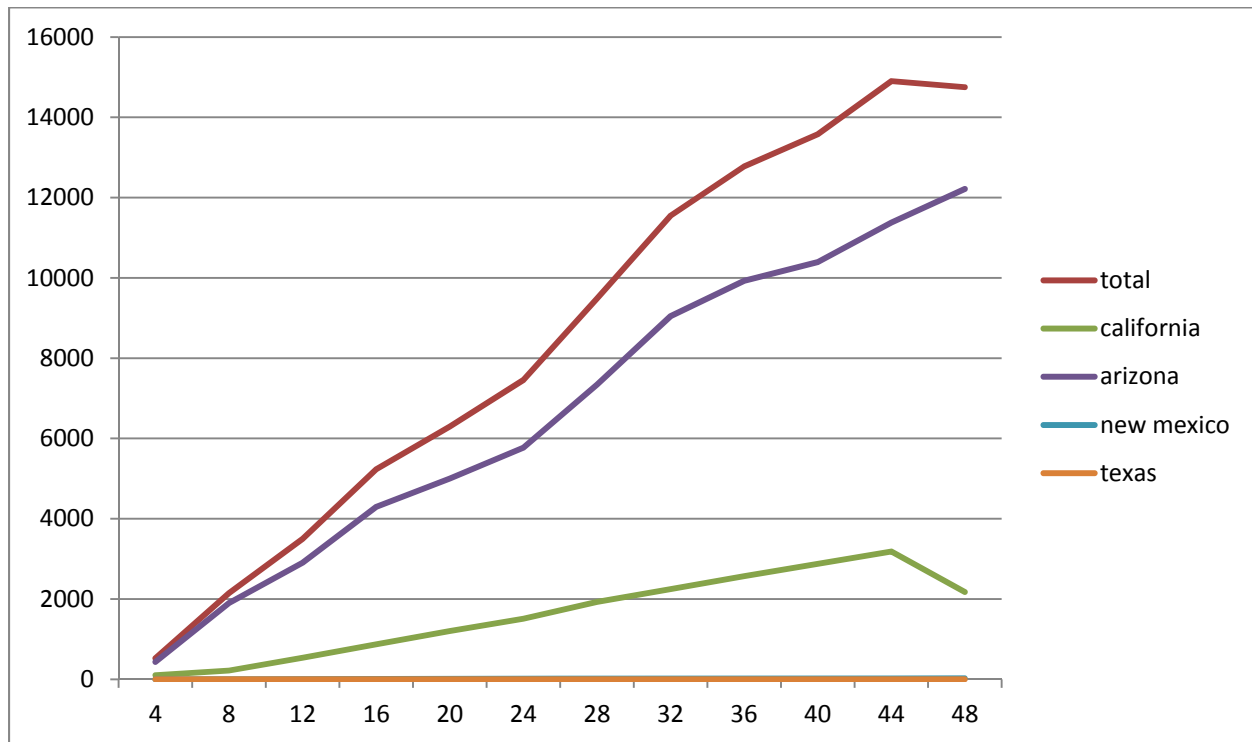


Figure 9. Endemic areas for Valley fever.

Arizona dust storms, also known as haboob, are a wall of dust as a result of a microburst or downburst. The air forced downward is pushed forward by the front of a thunderstorm cell, dragging dust and debris with it, as it travels across the terrain. These phenomena can disturb areas where the valley fever is in a dormant state and make it travel to new areas farther away.

Ideal dust sources occur in areas where the composition of the soil is very dry and loosely held on the surface. This most commonly occurs in arid and semi-arid regions, usually after a prolonged drought. Moisture keeps soil compact and helps maintain vegetation, which protects it from being swept up into passing winds. Not surprisingly, dust storms frequently occur in the desert. When wind passes over a dust source, the loosely held sand and dust particles move. When the soil is dry, it doesn't take much to get them moving. Additionally, the shifting winds cause turbulence and the high surface temperature creates convective currents at the leading edge

of the storm. These forces essentially act to lift particles higher and keep them aloft for longer. Since the diameter of the fungi is at the 2-4 micrometer, it is considered as an aerosol in the range between PM2.5 and PM10 (particulate matter).



Graph 1. Valley fever incidence in 2012

## Chapter 2

### Methodologies

For the first project, Comprehensive Air Quality Model with Extensions (CAMx) was used to evaluate ozone concentrations using the chemistry mechanism CB4 and CB5 on January 20<sup>th</sup>, 2011. The requirements for CAMx were meteorological files and emissions inputs. Weather Research Forecast (WRF) model was used to generate meteorological inputs and Sparse Matrix Operator Kernel Emissions (SMOKE) model was used to convert low level emissions at a yearly basis to model emissions could be used on an hourly setting. During those simulations, the map projection was centered on El Paso, Texas as lambert conformant and the WRF model ran at 35 sigma vertical levels. Data from WRF was converted using Community Multiscale Air Quality (CMAQ), starting with MCIP (meteorological coupling interface processor), BCON (boundary conditions) and ICON (Initial conditions) files in order to have those parameters ready for CAMx. Also, WRF meteorological data was converted to CAMX friendly format using a script provided by ENVIRON.

The CAMx models was run on three domains with a 36km, 12km and 4km resolution and were spanned over the entire troposphere and lower stratosphere in order to get ozone concentrations.

Ozone data for model evaluation and comparison were taken from the Texas Commission for Environmental Quality (TCEQ) monitoring stations, this allowed experimental data to be compared against simulated data.

For the second project, the ozone concentrations of 8 hour average were taken from monitoring stations on the areas of downtown Los Angeles, Azusa, Pomona, Upland, Riverside-Rubidoux and Crestline-Lake Gregory. Those areas represent different height, upwind, downwind, and terrain topology. Future trends in NO<sub>x</sub> and VOC mixing ratios were estimated on expected changes in emissions from 2010 to 2030. CMAQ model simulations for a baseline 2008 and 2030 using meteorological and emission inputs from the South Coast Air Quality Management District (SAQMD) in order to develop a 2012 air quality management plan. The grid resolution was at 4km and the center location varied as it was positioned at every station mentioned on Los Angeles, Azusa, Pomona, Upland, Riverside-Rubidoux and Crestline-Lake Gregory coordinates. The chemistry mechanism used was SAPRC99 photochemical, 5 aerosol module and saprc99\_ae5\_aq aqueous chemistry. For the simulation, the CMAQ code was compiled in MPICH to run in distributed computing using 96 cores, optimizing the time of each run.

Both initial (ICON) and boundary (BCON) conditions were defined using a profile file. The default ICON and BCON profiles have been developed for the Regional Acid Deposition Model (RADM2) chemical mechanism and the terrain following sigma-p coordinate system. Both the initial and boundary condition profiles are intended to represent relatively clean air conditions in the eastern-half of the United States, and have been formulated from available measurements and results obtained from modeling studies. Thus, they do not represent any specific time period. The predefined profile data are stored in ASCII files in the CMAQ system. The ICs and BCs generated by these two processors are used by the CMAQ Chemical Transport Model (hereafter referred to as the CCTM).



The ICON and BCON processors generate initial and boundary conditions for individual model species, which include gas-phase mechanism species, aerosols, nonreactive species and tracer species.

The CCTM will attempt to extract initial and boundary conditions for each species being modeled from the input files. The solution of partial and ordinary differential equations that arise in air quality models requires both initial concentrations and boundary conditions. The ICON processor generates species concentrations for every cell in the modeling domain, whereas the BCON processor generates species concentrations for the cells immediately surrounding the modeling domain (Gipson).

For multiday simulation profile files were used to initialize the model and the output of each day worked as initial condition for the next day. The simulation were compared to the SCAQMD 2008 baseline for 91 days of summer to correlate error, and successfully reproduced the results, then adjustments to 2008 and 2030 emission inputs were taken to forecast the effects of varying incremental NO<sub>x</sub> reductions and VOC underestimation emissions. Sensitivity simulations were performed to determine if the model improved by factors of 1.5 and 2.0 on VOC and supplemental sensitivity simulations were included to allow more detailed data on NO<sub>x</sub> and VOC response on ozone emission.

For the third project, two events were recorded by the USGS (United States Geological Survey) to be dust storms with those meteorological characteristics, one on April 14th 2012. In order to check the wind vector, Hysplit was run on forward mode on Phoenix, AZ (33,-112) and El Paso, TX (31,-106) coordinates and correlated with Plymouth State Weather Center Contoured Maps for Archived Data on wind vector and visibility. Also, data from modis terra 1000m satellite image was used to verify dust presence in the area and experimental data was taken from TCEQ (El Paso Area) and Envista (Tucson Area).

Weather research Forecast (WRF) was used to reproduce the meteorological conditions for both events, such as temperature, wind speed and direction, pressure, planetary boundary layer height, humidity and others. The first step was to obtain the WRF inputs from National Centers for Environmental Predictions (NCEP) Operational Model Global Tropospheric Analyses on grib2 format for the event days. Again, data from WRF was converted using CMAQ, starting with MCIP (meteorological coupling interface processor), BCON (boundary conditions) and ICON (Initial condition) files in order to have those parameters ready for CAMx. Also, WRF meteorological data was converted to CAMX friendly format using a script provided by ENVIRON. WRF was optimized and compiled to run on 76 cores increasing the speed of the simulations.

Emission processor system 3 (EPS3) was used to simulate a dust storm emission and its source area, as well as the dimension and the quantity and comprehensive air quality with extensions (CAMx) model in inert mode to simulate the dispersion from the source emission (AZ) to the destination area (TX). Also, as well as WRF, CAMx was compiled with MPICH to run on 76 cores increasing its performance and speed. The result was displayed using a visualizer program called Verdi to compare the simulated data against satellite images. Lastly, planetary

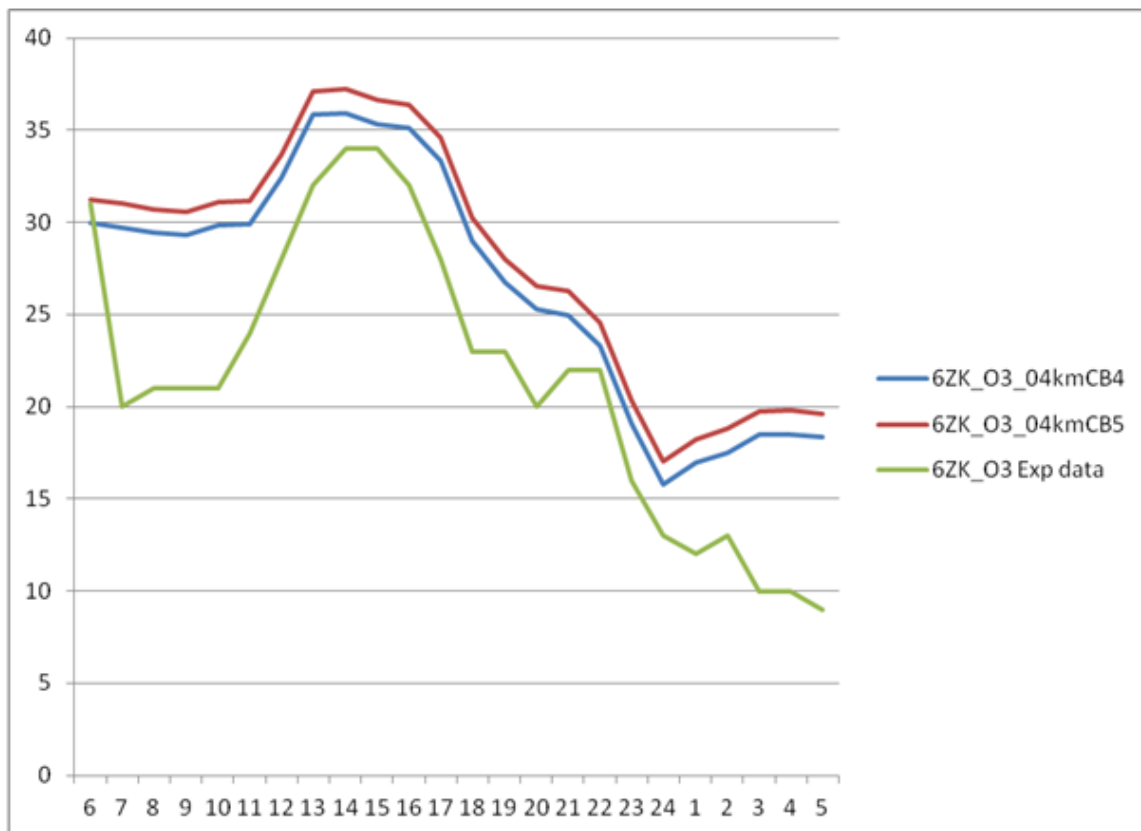
boundary layer height (PBLH) was extracted from WRF and compared against University Wisconsin sounding files in skew-t.

## Chapter 3

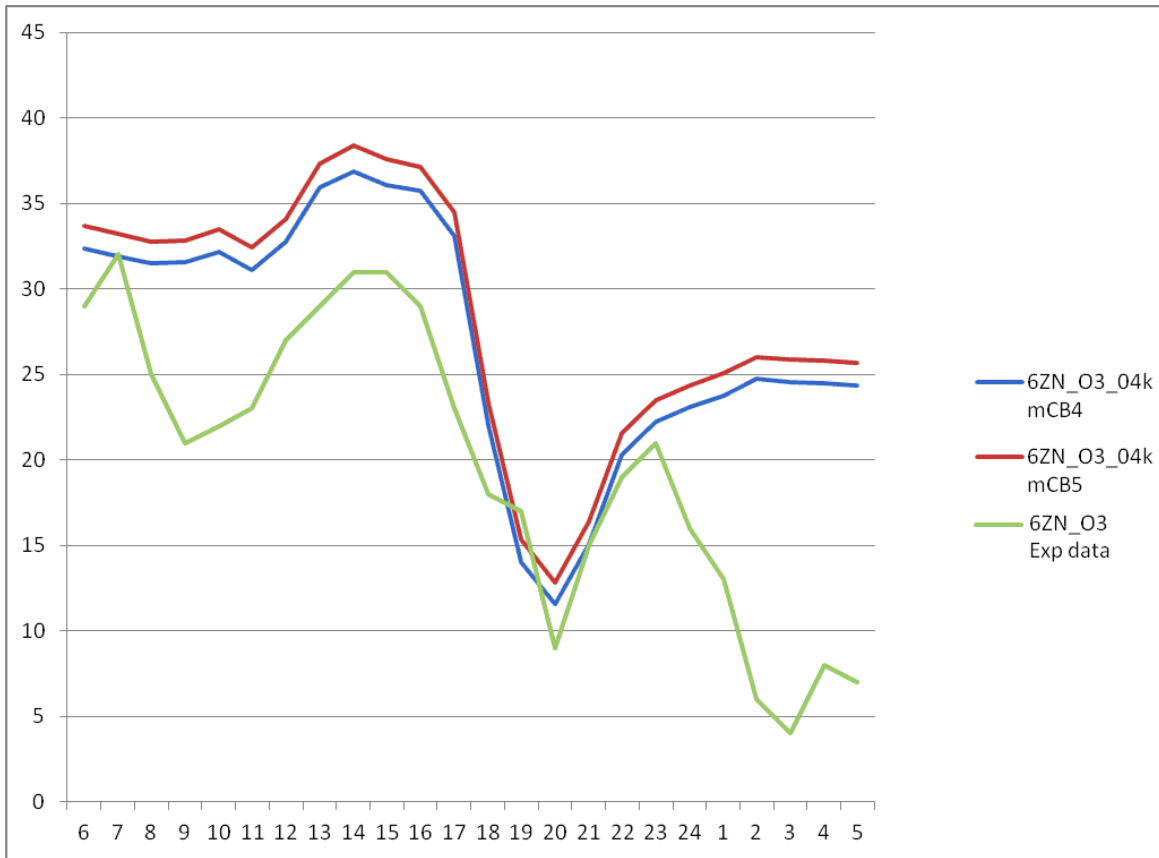
### Results

For the first project, the results for the ozone concentrations for the simulations of CB4 and CB5 were correlated and the shared variance was near unity.

The simulated ozone concentrations for both mechanism was greater than the measured data at the stations, this indicate that neither would pass the US Environmental Protection Agency standards for the state implementation planning at all stations. The mean normalized error for the simulations is not less than 35% and the normalized bias is greater than 15%, which is very high.



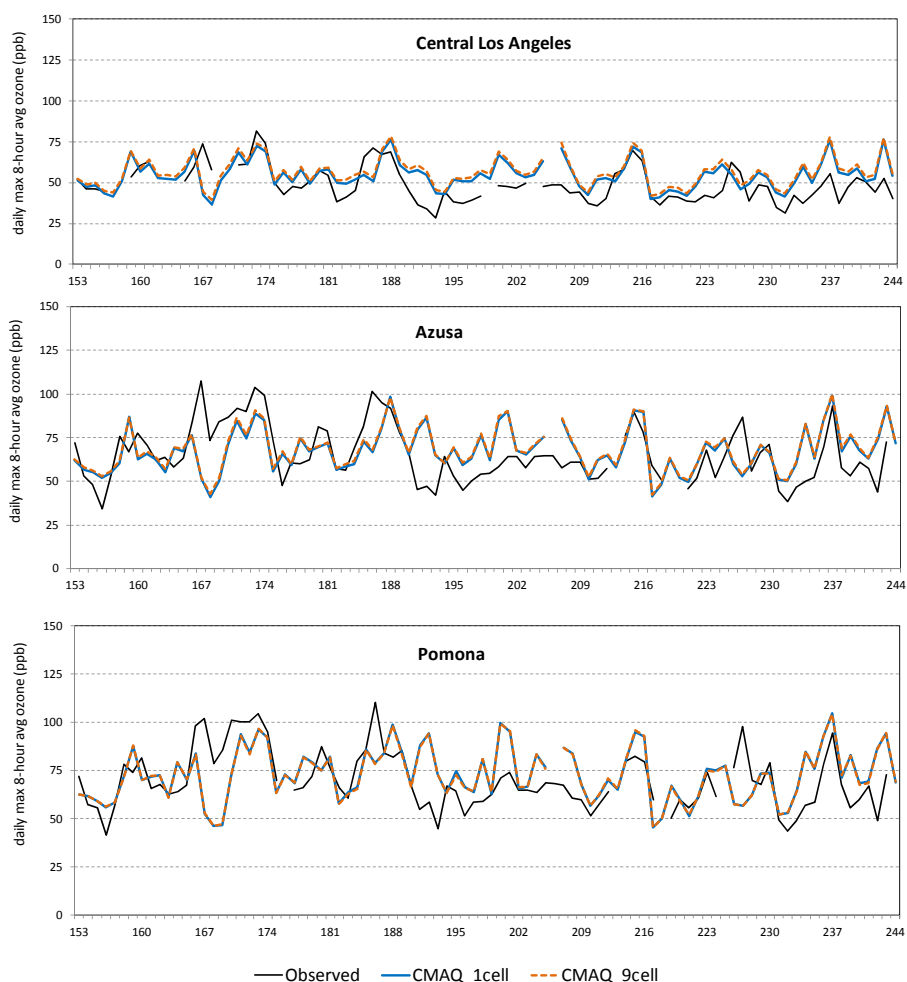
Graph 2. Results from station 6ZK



Graph 3. Results from station 6ZN

For the graphs shown above, the blue line represents the simulated data using CB4, the red line represents the data simulated using CB5 and the green line is the experimental data taken from the corresponding station, in this case 6ZK (Chaparral) and 6ZN (Santa Teresa). The simulations reproduced the high mixing ratios but not the lower mixing ratios; both reported a behavior of a drop during the early morning hours and then drop to almost zero during the late evening. However, it did not follow the trend of the experimental data at early hours.

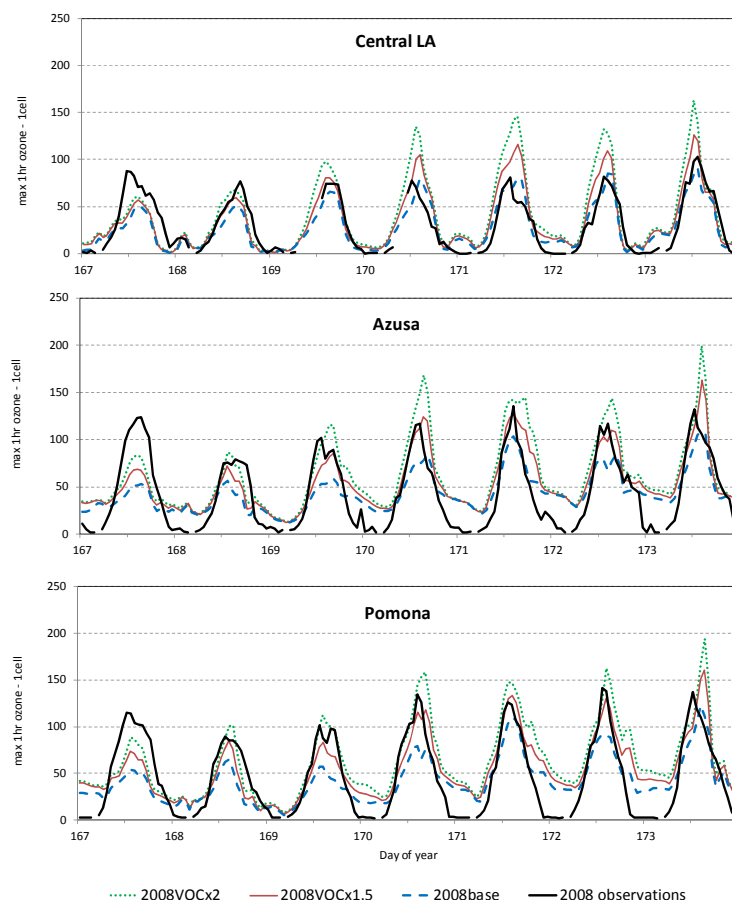
For the second project, the simulations for the base year 2008, included 91 days from June through August; where it included seven multiday ozone episodes. The model results obtained were identical to those obtained by the SCAQMD, so the simulations were well correlated for the 2008 cases for one-hour daily maximum ozone rate for the 91 days. The model evaluation was divided in three zones, Zone 3 which included the San Fernando Valley, Zone 4, the eastern San Gabriel, Riverside and San Bernardino valleys and Zone 5, the Los Angeles and Orange County areas. The CMAQ ozone simulations meet the 1-hour average unpaired peak and normalized error model performance goal in all three zones on most days. Zone 4 has the maximum ozone concentration and is the primary downwind impact zone as well as it displayed the best unpaired peak performance with 54 out of 58 days meeting the 20% criteria. Zone 5 showed a tendency of over prediction in all 90 days and Zone 3 lagged the unpaired peak performance with 79% of the days meeting the criteria.



Graph 4. CMAQ vs Observed simulation for base 2008.

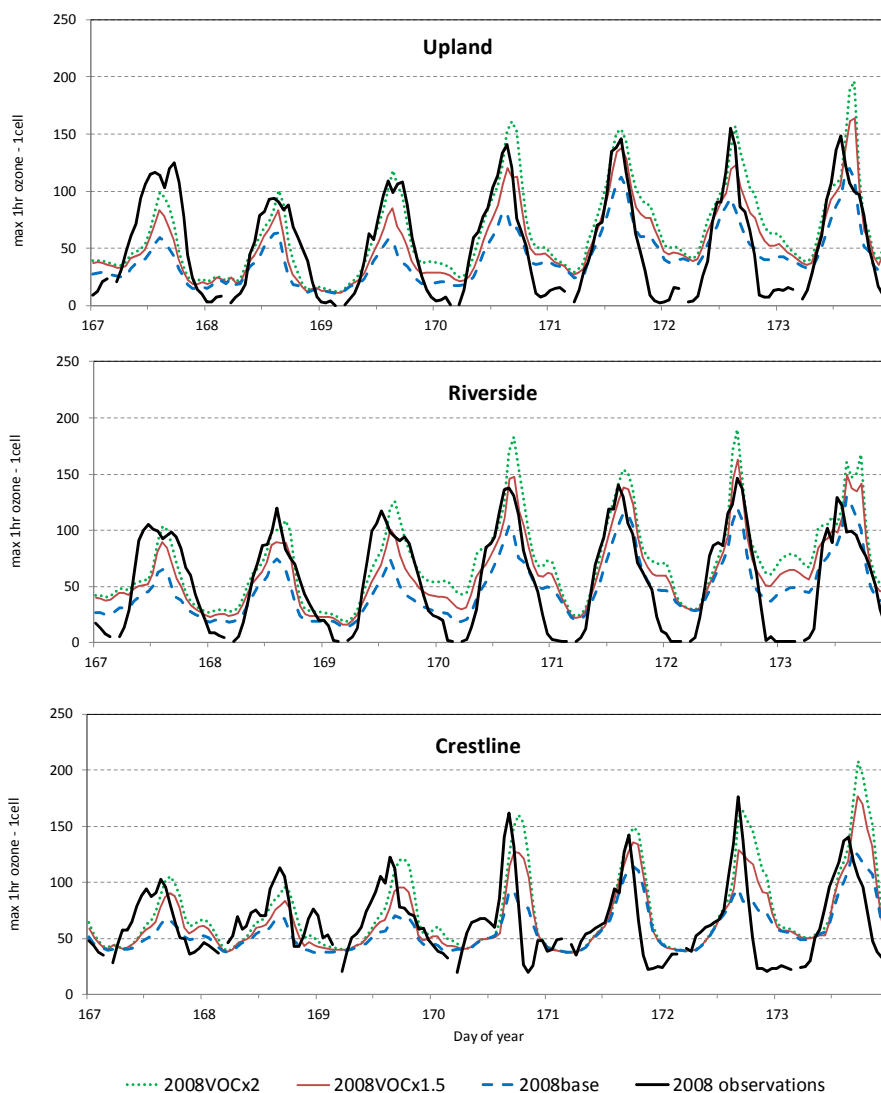
Also, two additional sets of simulations were performed for the 2008 base year to simulate the effect of increasing VOC emissions by a factor of 1.5 and 2.0 on the inputs. The objective was to determine whether upward adjustments on 2008 base VOC inventory yield a better result between observed and predicted ozone values at Los Angeles, but under predicts the observed ozone values at other sites. Adjustments by factors of 1.5 and 2.0 results in predicted ozone values that are  $1.19 \pm 0.28$  and  $1.39 \pm 0.35$  times higher, respectively, than the observed values at Los Angeles. A factor of 1.5 adjustment results in good agreement for the other five sites with

average observed/predicted ratios of  $0.98 \pm 0.2$  for 1-hour ozone and  $1.00 \pm 0.2$  for the 8-hour ozone, and a factor of 2.0 result in over prediction with ratios of  $1.18 \pm 0.22$  and  $1.17 \pm 0.22$  for 1-hour and 8-hour ozone, respectively. These results combined with the findings of the 2010 Van Nuys Tunnel Study (Fujita et. al., 2012) and the most recent top-down emission inventory evaluation (Fujita et al., 2013) support the conclusion that VOC emissions in the 2008 base inventory are underestimated and that the 2008 total VOC emissions should be increased by a factor of 1.5 or on-road mobile VOC emissions only by a factor of 2.



Graph 5. CMAQ simulations with factors of 1.5 and 2.0 VOC against 2008 base and observed values.





Graph 6. CMAQ (Continued) simulations with factors of 1.5 and 2.0 VOC against 2008 base and observed values.

The indications that current estimates of VOC emissions may be underestimated relative to NOx emissions have important implications for modeled demonstrations that the selected emission reductions will result in ambient concentrations that meet the NAAQS. Attainment is demonstrated using the relative reduction factors (RRF), which are the ratios of the model's future to current (baseline) predictions at monitoring locations.

In regions that are VOC limited with respect to ozone formation, such as the SoCAB, an underestimation of VOC emissions in the base year will result in lower predicted ozone and higher RRFs. Correcting the underestimation will yield a lower RRF and decrease the emission reduction necessary to demonstrate attainment. In other word, underestimation of base year emission will result in overestimation of required emission reductions.

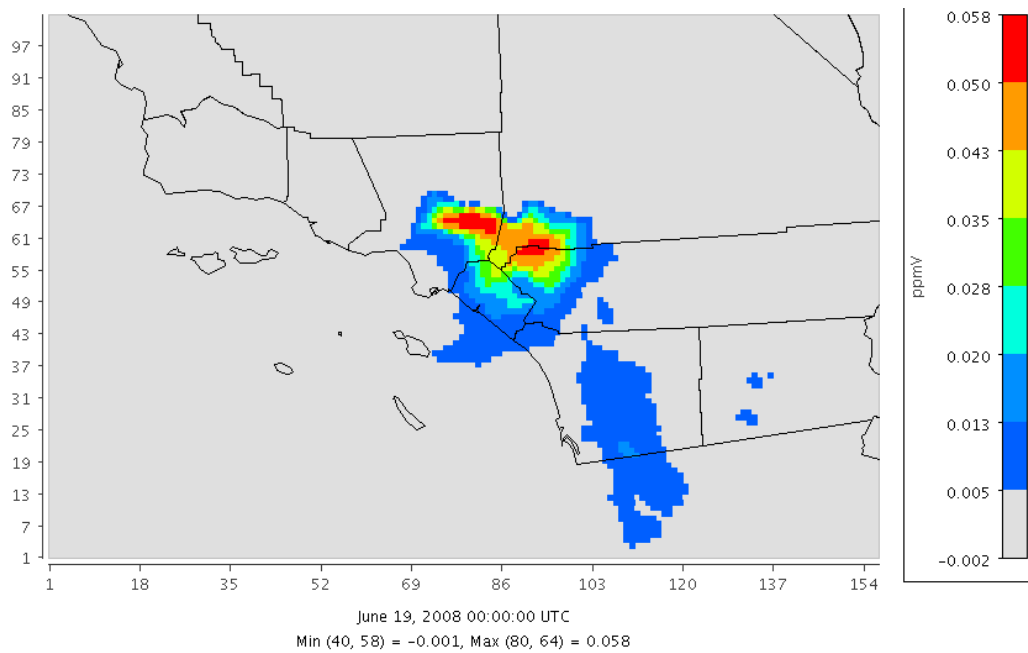


Figure 10. Contour plot of 2008 VOC1.5 - 2008 Base

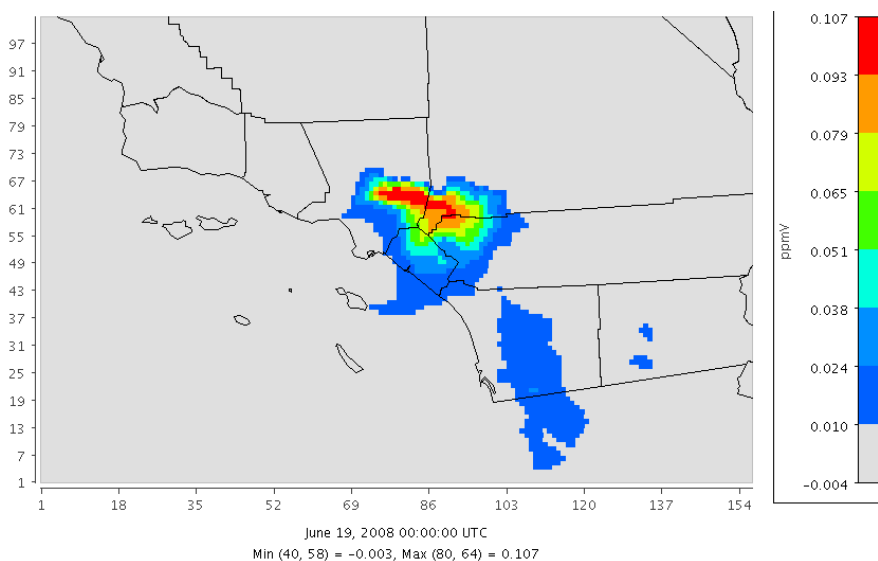
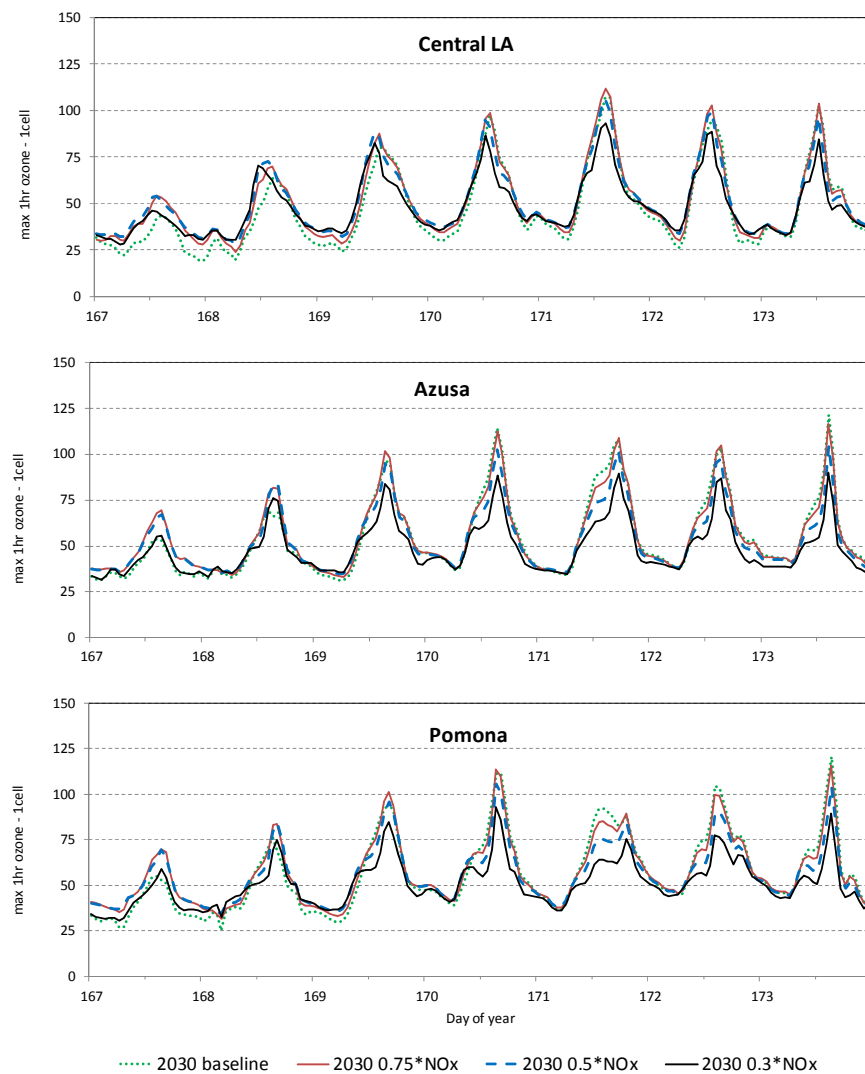


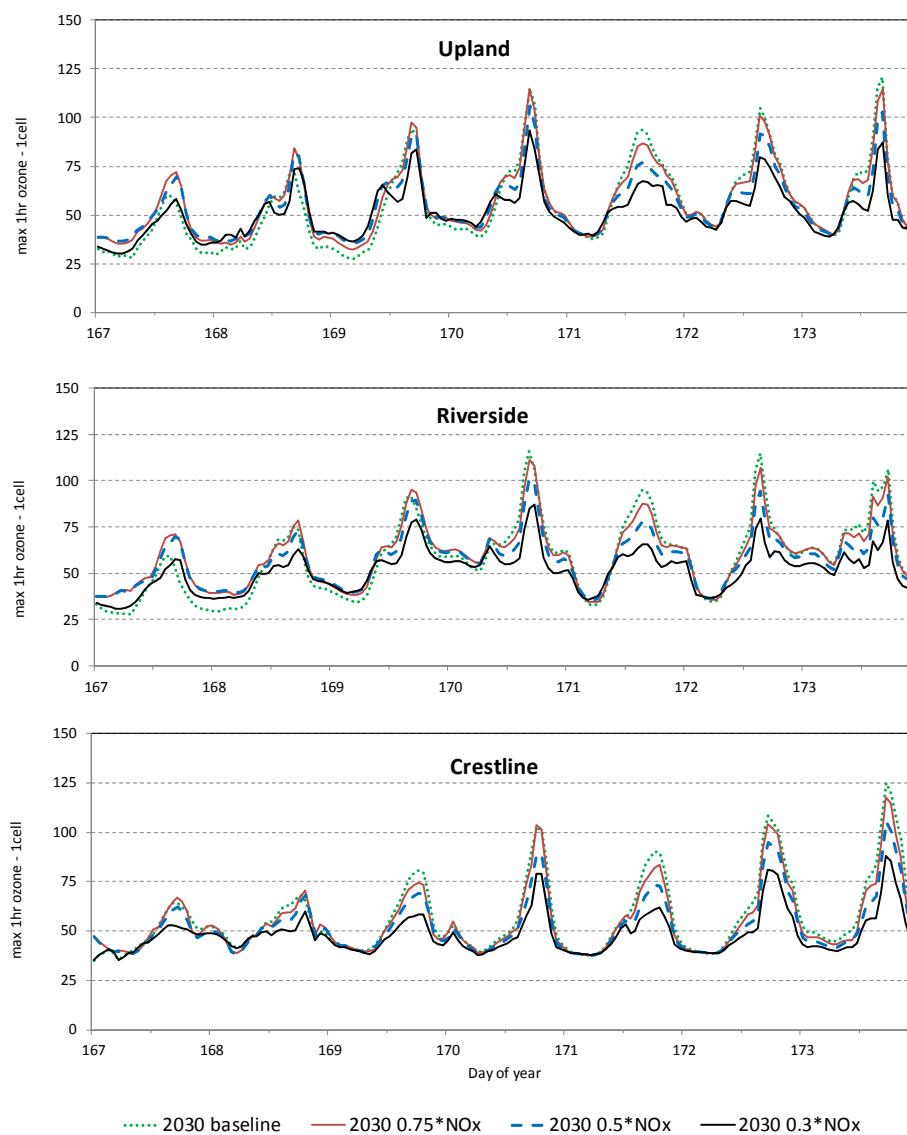
Figure 11. Contour plot of 2008 VOC2.0 - 2008 Base

The results for 2030 simulations are consistent with our earlier prediction of increasing ozone trends in the central and western basin with a shift of the peak ozone levels from the far eastern portions of the basin in the San Bernardino Mountains westward toward the more populated area of the basin (Fujita et al., 2013). With 2030 baseline NO<sub>x</sub> emissions and 2030 baseline VOC emissions, the average daily maximum 8-hour ozone concentrations are predicted to increase by 18, 14, 11 and 10 percent at Los Angeles, Azusa, Pomona and Upland, respectively, and decrease by 2 and 4 percent at Rubidoux and Crestline, respectively. Ozone levels are not significantly different with 70% reduction in NO<sub>x</sub> emissions except for further marginal decreases in the eastern basin. At 81% reduction in NO<sub>x</sub>, the average 8-hour ozone concentration at Los Angeles remains about 18% higher than 2008 levels and most of the central basin remains at 2008 levels. However, ozone levels at Rubidoux and Crestline are predicted to be 13 and 17 percent lower, respectively, relative to 2008 levels and the basin site shifts to the central basin. With 88% reduction in NO<sub>x</sub>, ozone levels at Azusa, Pomona, Upland, Rubidoux

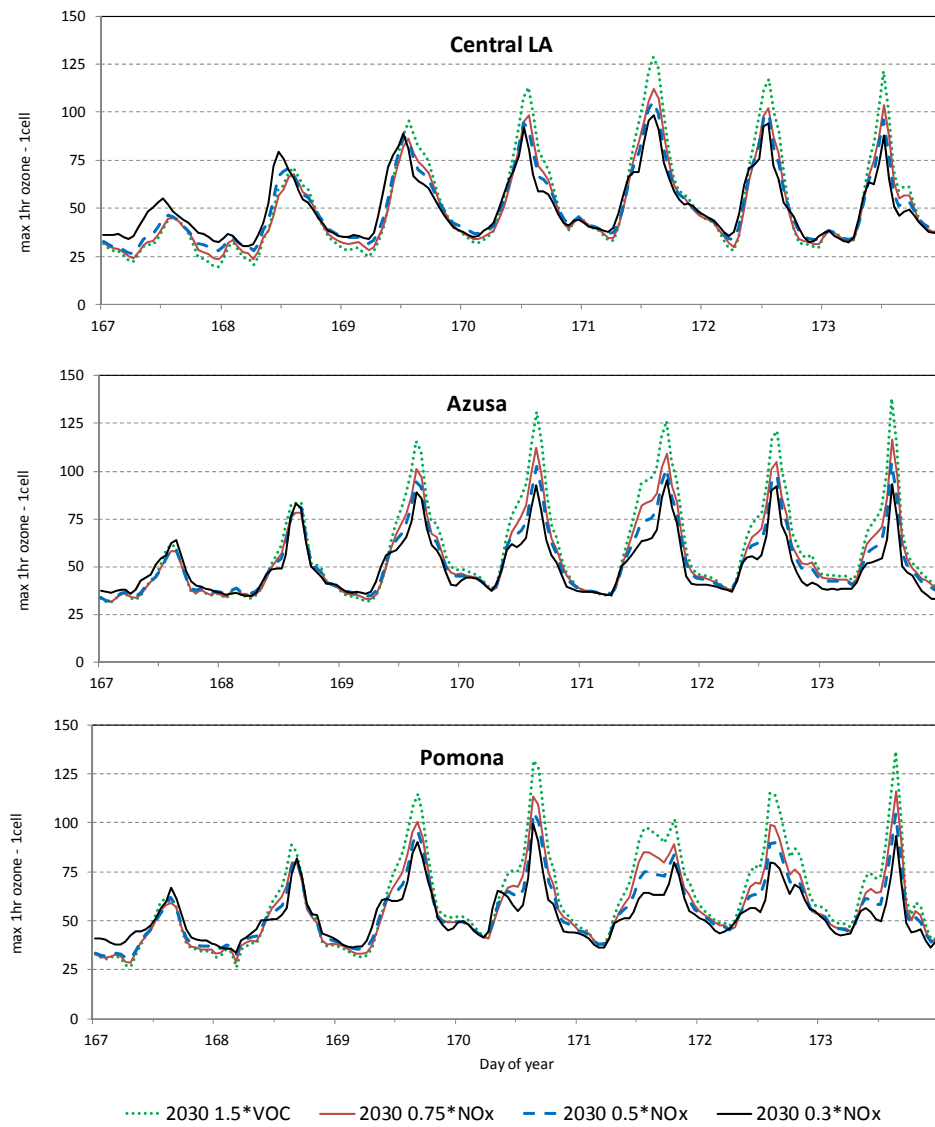
and Crestline are decreased by 8, 12, 13, 24 and 27 percent from 2008, respectively. If 2008 base ROG emissions are underestimated by 50%, ozone levels are reduced by about 30% at all sites in the basin with 2030 baseline VOC and NO<sub>x</sub> remaining at 2008 levels. NO<sub>x</sub> reductions are counterproductive or ineffective in the western and central basin even with 88% reduction. Only the eastern basin show marginal further reduction in ozone.



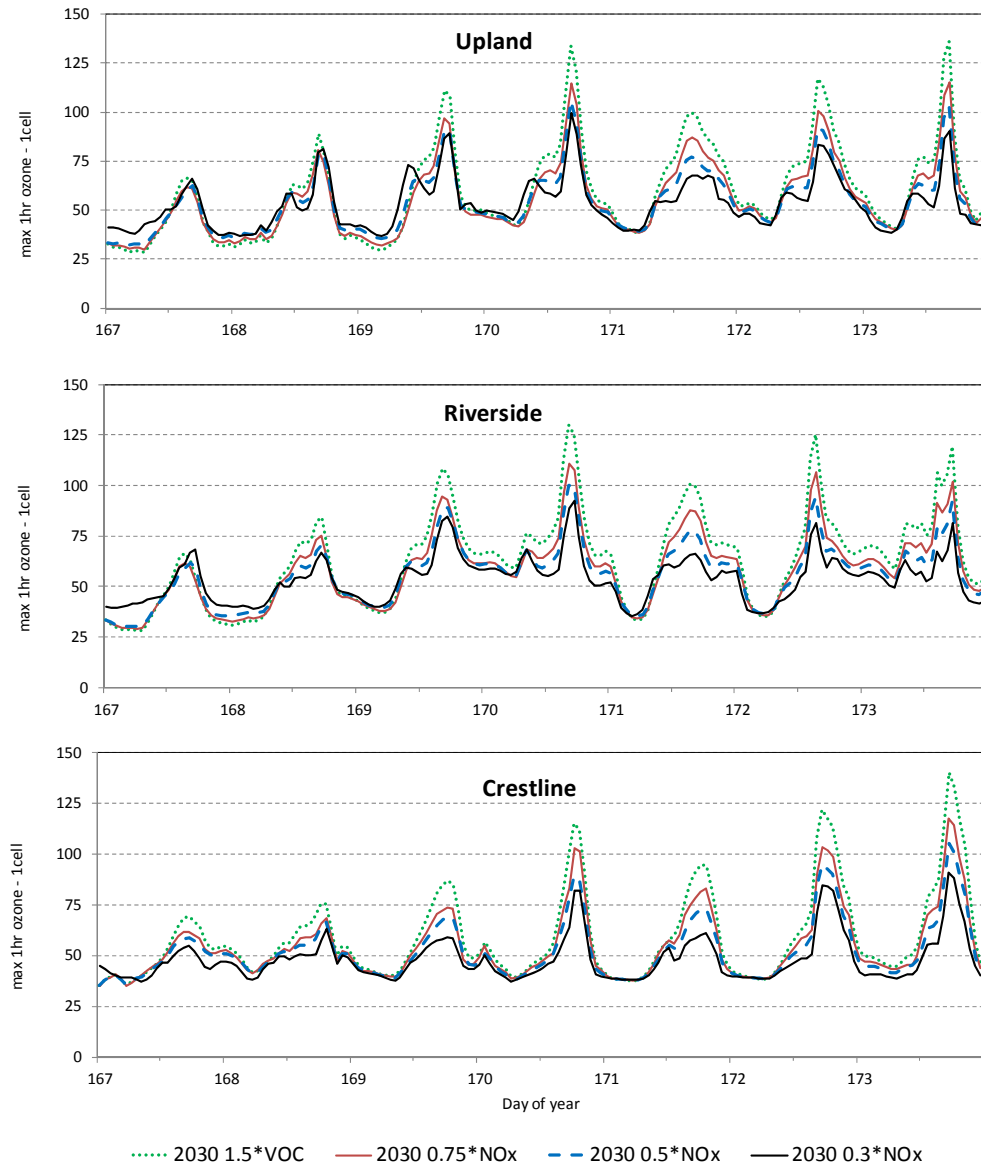
Graph 7. CMAQ simulations with factors of 0.75, 0.50 and 0.30 NO<sub>x</sub> against 2030 base.



Graph 8. CMAQ (Continued) simulations with factors of 0.75, 0.50 and 0.30 NOx against 2030 base.



Graph 9. CMAQ simulations with factors of 0.75, 0.50 and 0.30 NOx against 2030 base with 1.5 of VOC.



Graph 10. CMAQ (Continued) simulations with factors of 0.75, 0.50 and 0.30 NO<sub>x</sub> against 2030 1.5 VOC.

Using the relative response factors (RRF) referenced to the 2008 simulations with base ROG emissions, all projected design values will exceed the ozone NAAQS even with 88% NO<sub>x</sub> reduction. DVs for the western and central basin are projected to be equal to or higher than 2008 levels with 50% reduction from 2030 baseline. If 2008 base VOC emissions are underestimated

by 50% (i.e., VOC reductions from 2008 of -54% rather than -32%), all sites except Crestline show attainment with NOx emissions remaining at 2008 levels. Close to 90% reduction in NOx would be required to show attainment at Crestline. Failure to reach 90% NOx reduction would leave the central basin in nonattainment of the ozone NAAQS due to NOx disbenefit.

The preliminary ozone modeling analysis by the SCAMD for the 2012 AQMP (SCAQMD, 2013) projected that reductions in NOx emissions from 2010 levels of 90% would be required to attain the 2008 8-hour ozone NAAQS of 75 ppb by 2032. This level of reduction is equivalent to a basin NOx carrying capacity of roughly 80 tpd. While our results are generally consistent with SCAQMD's preliminary assessment that reductions in NOx emissions of about 90% would be necessary for attainment of the 8-hour ozone NAAQS, they demonstrate that uncertainties in the base year ROG emissions can greatly affect the projected NOx reductions needed to show attainment.



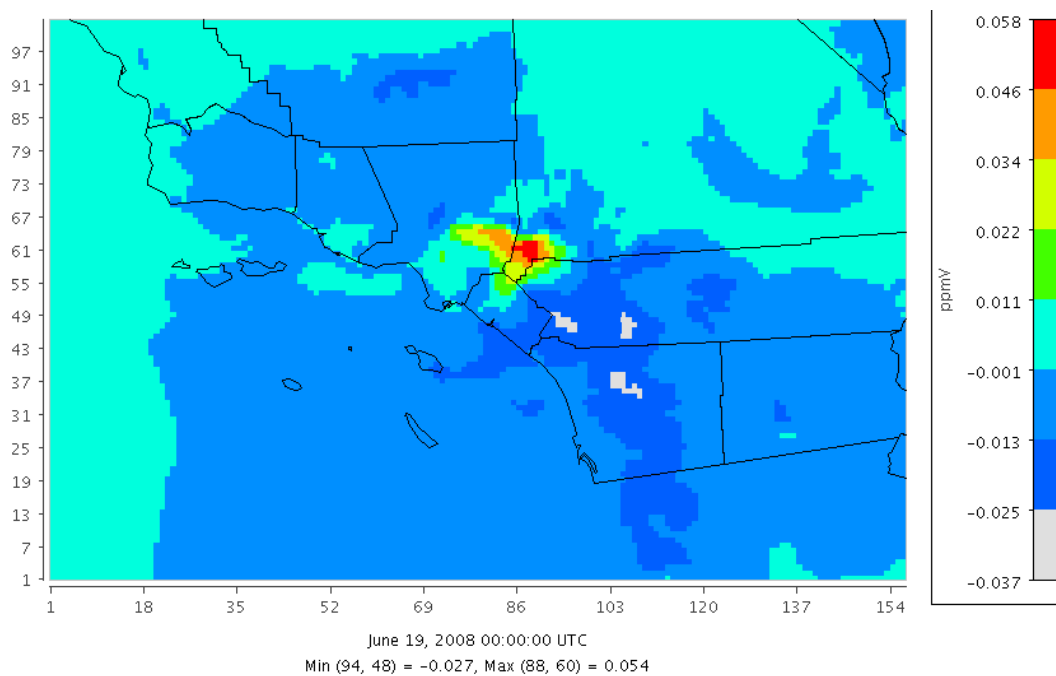


Figure 12. Contour plot of 2030 base – 2008 Base

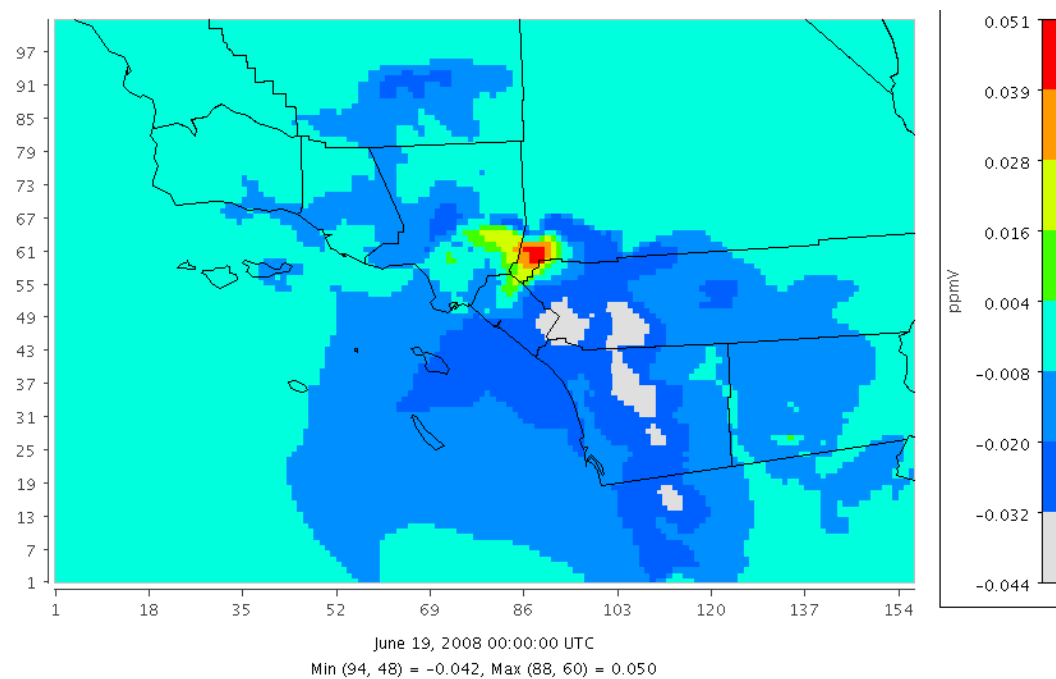


Figure 13. Contour plot of 2030 NOx 0.5 – 2008 Base

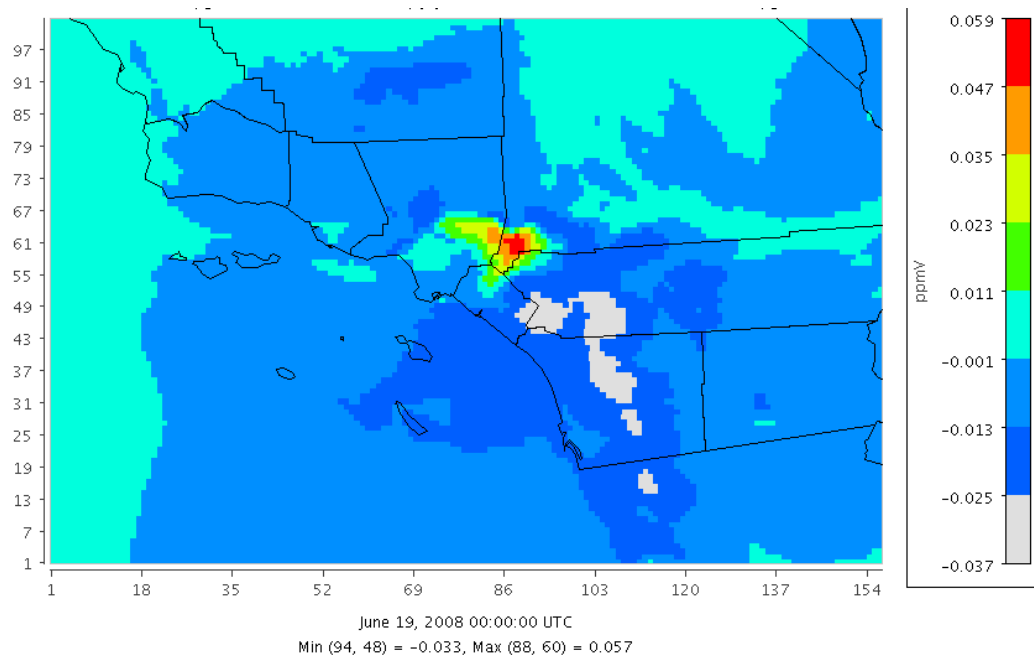


Figure 14. Contour plot of 2030VOC10NOx0.75 - 2008 Base

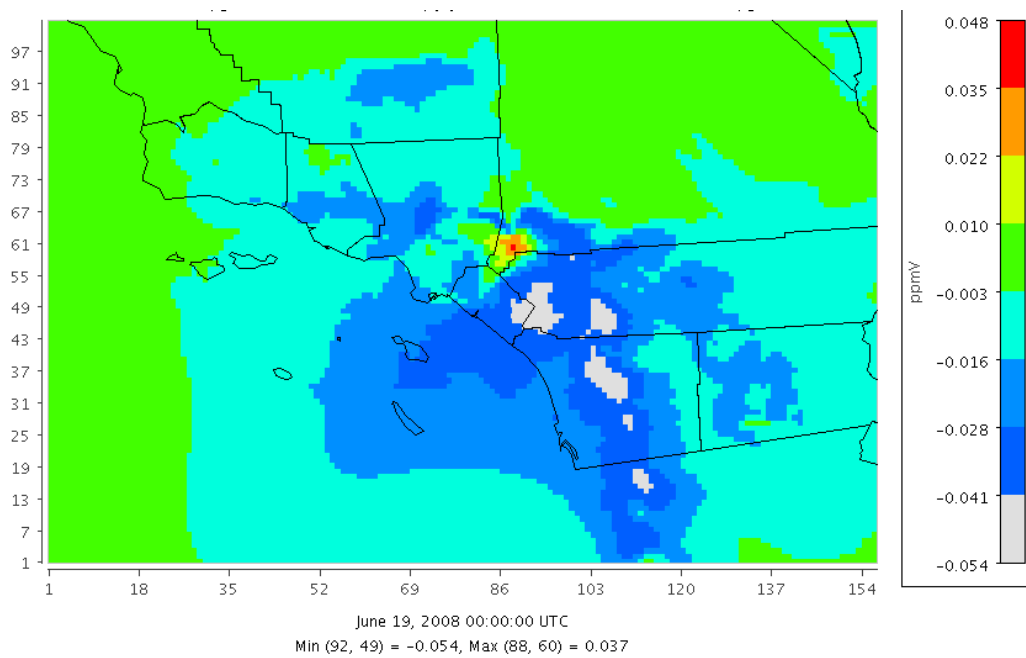


Figure 15. Contour plot of 2030NOx0.3 - 2008 Base

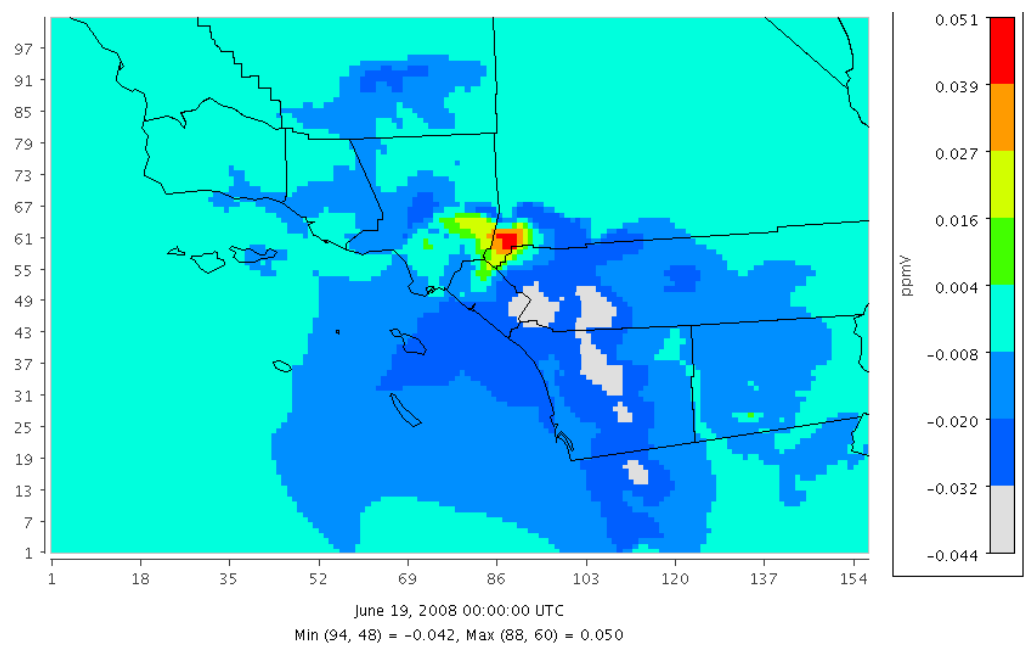


Figure 16. Contour plot of 2030VOC1.5NOx0.5 - 2008 Base

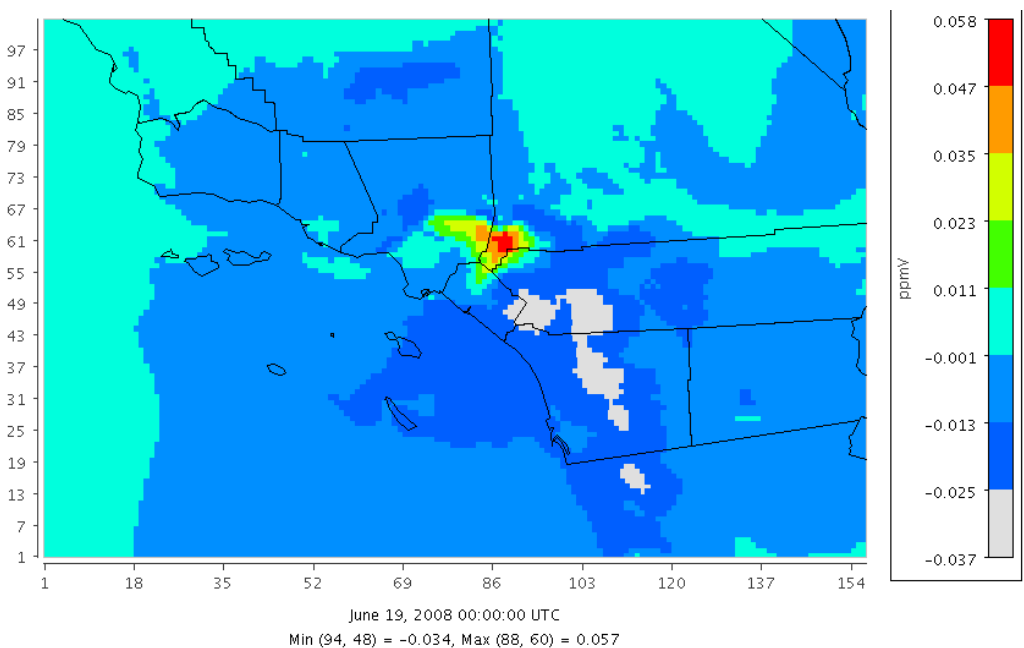


Figure 17. Contour plot of 2030VOC1.5NOx0.75 - 2008 Base

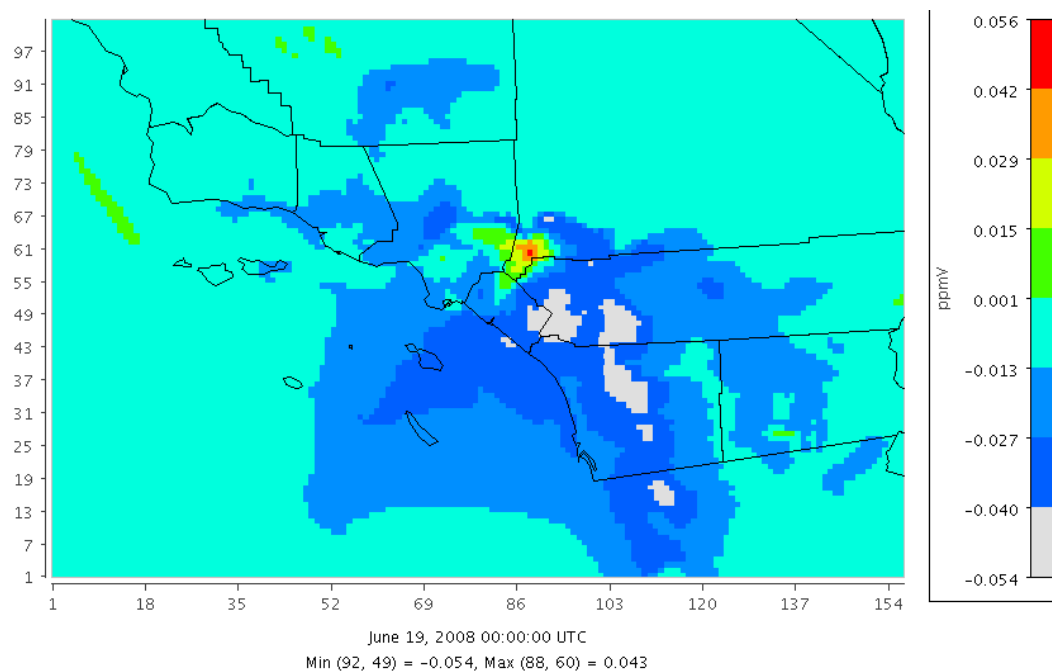


Figure 18. Contour plot of 2030VOC1.5NOx0.3 - 2008 Base

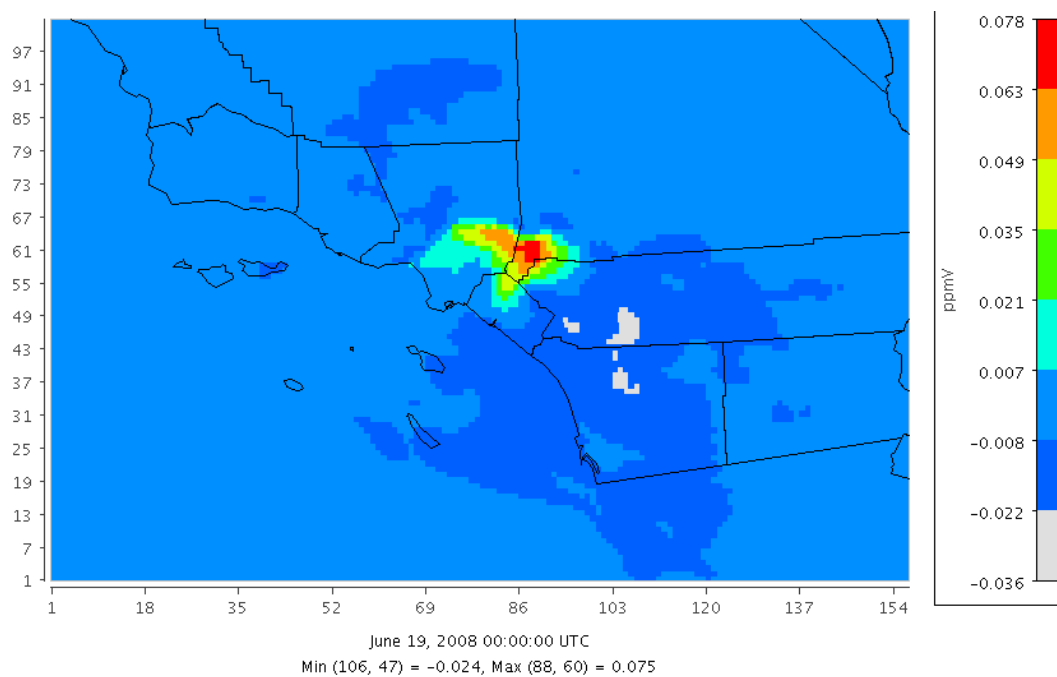


Figure 19. Contour plot of 2030VOC1.5NOx1.0 - 2008 Base

For the third project, the analysis of the April 14<sup>th</sup> 2012 was made in experimental data from stations and simulated output from CAMx.

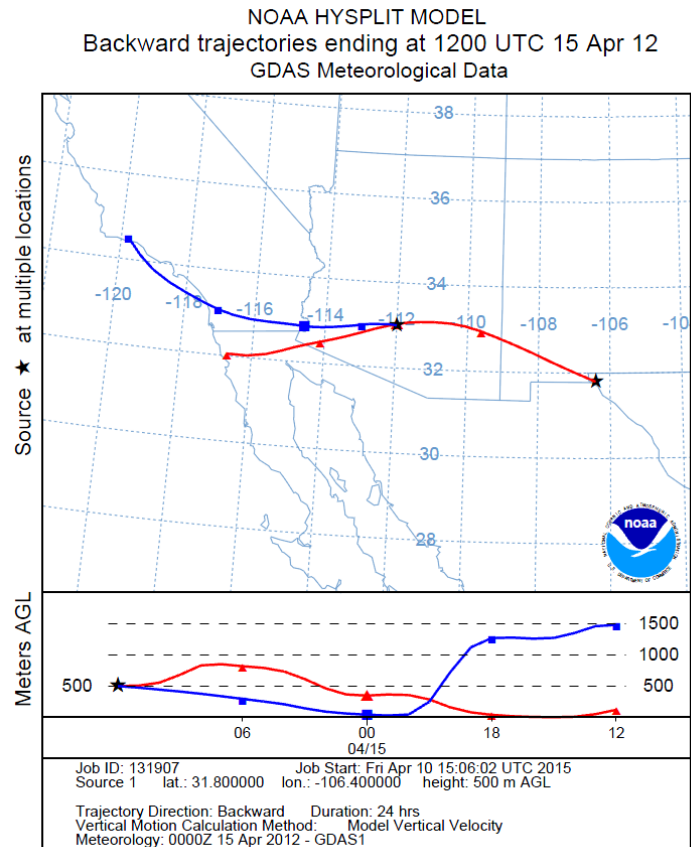


Figure 20. Hysplit result of the dust event

The hysplit graph on backward mode was set to the points -112,33 which correspond to the Phoenix Area and -106,31 to El Paso, respectively. The direction of the wind is shown to travel directly from the source area in Phoenix to the destination in El Paso, with altitudes of 500 meters above ground level at the source and descending almost to 0 at the destination. The airspeed was correlated with the program Windrose which showed most of the wind direction from the west at an average speed of 22 and 11 knots.

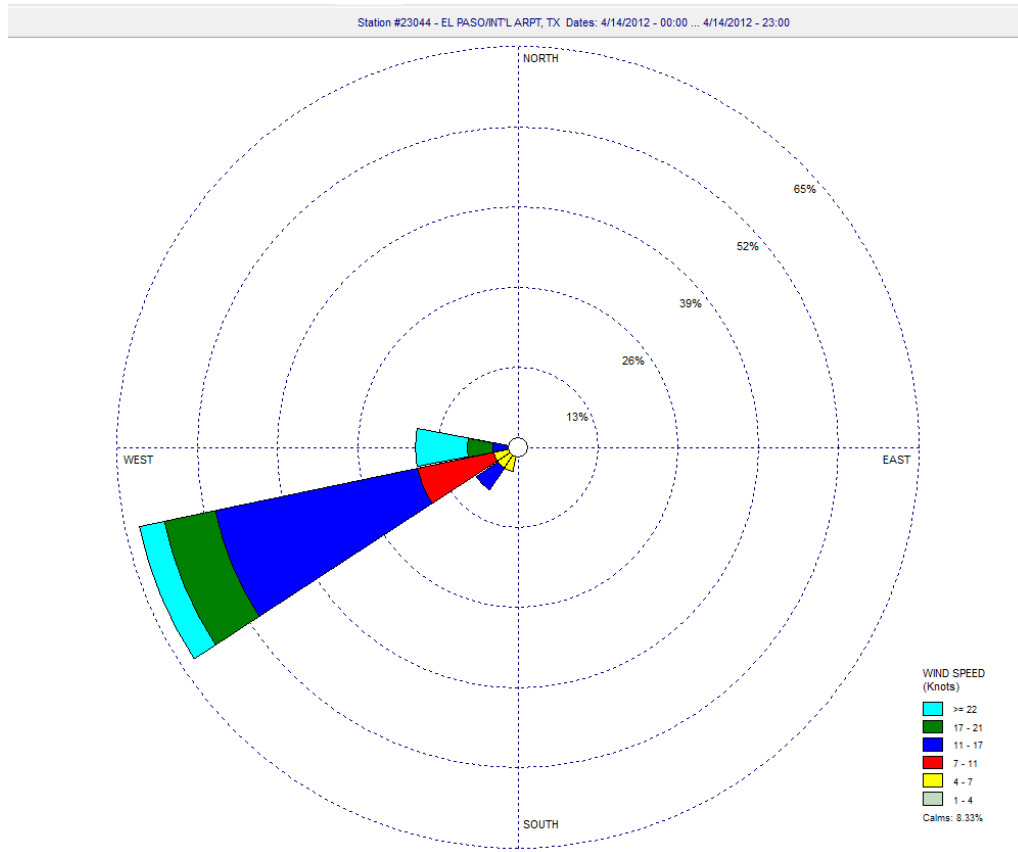


Figure 21. Windrose result of the Dust event

In order to verify a dust storm, the satellite image taken from MODIS terra (MODIS terra products), clearly has shown a dust plume approaching El Paso area. The pattern is visible traveling from west-southwest, and the event spanned from 1:00 pm MST until 6:00 pm MST. The event had three parts, which started in a rise of dust storm condition between 1pm and 2pm, a sustained dust storm between 3pm and 4pm and a final phase from 5pm and 6pm.

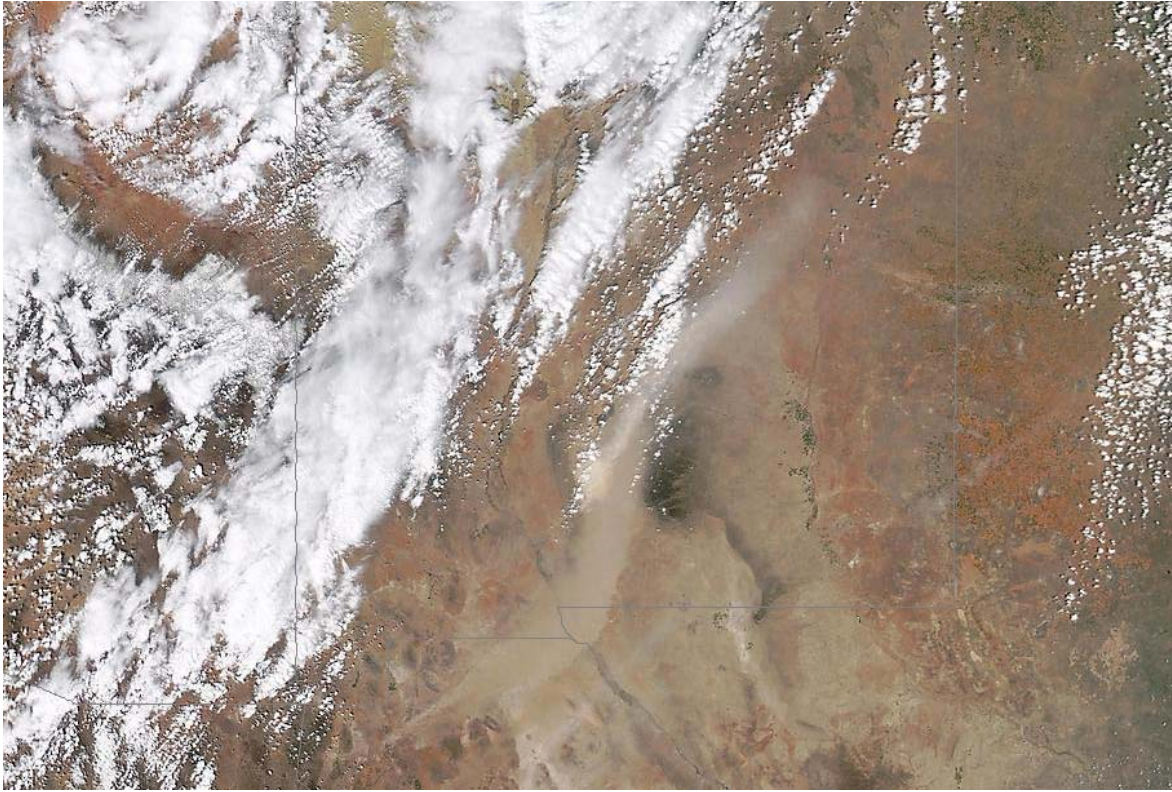


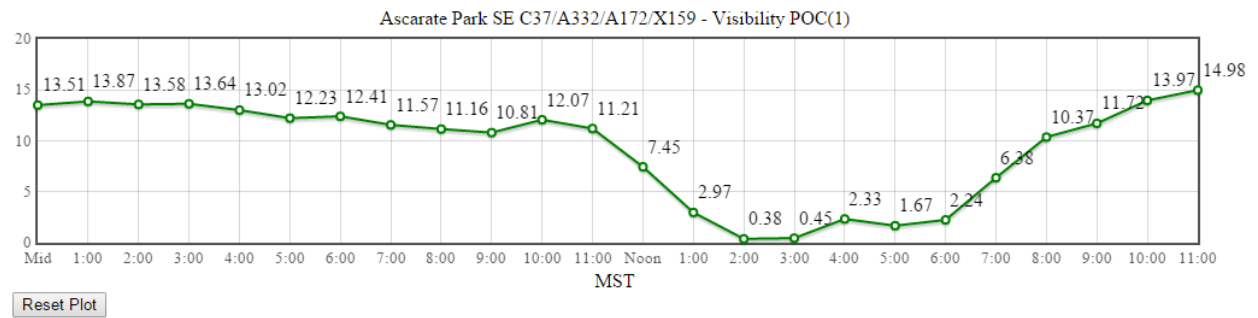
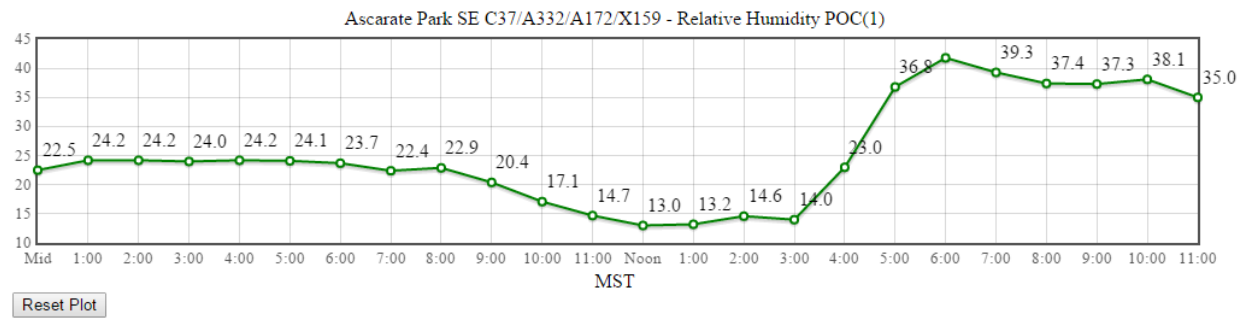
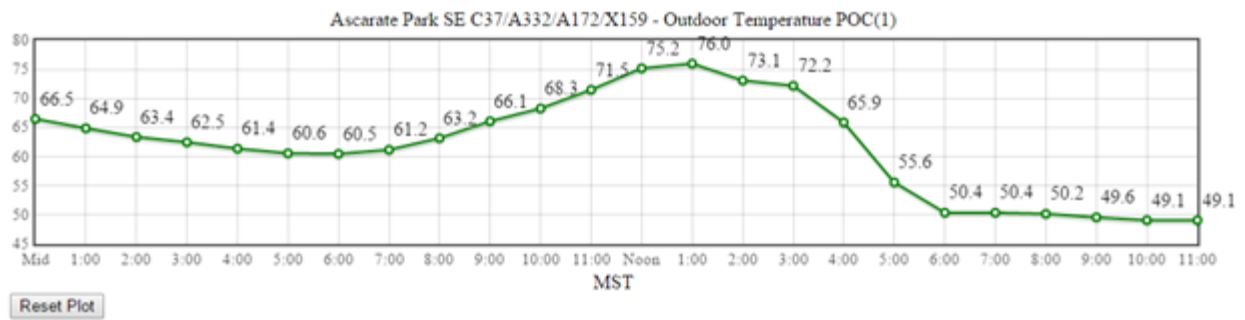
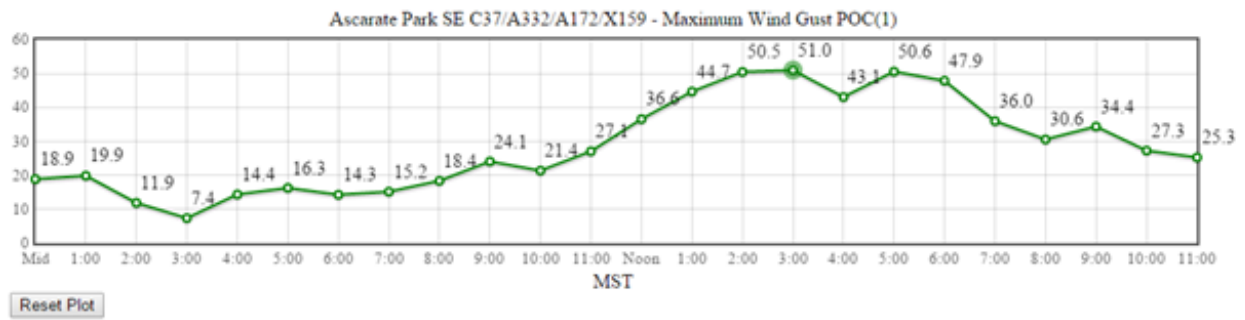
Figure 22. Satellite image of the dust storm.

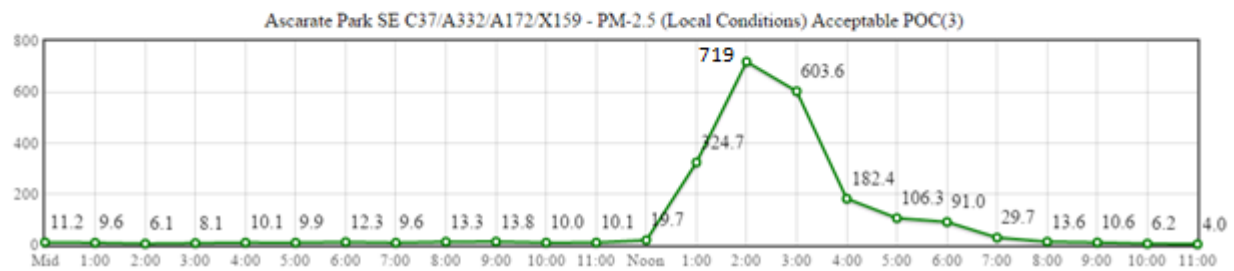
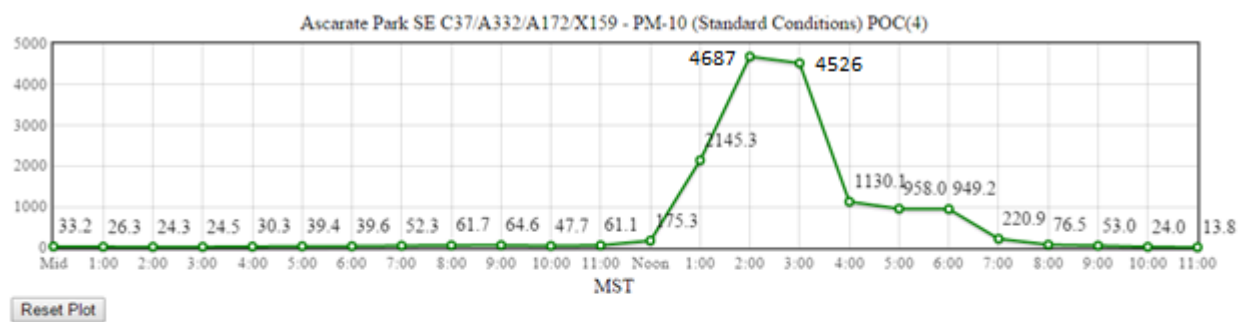
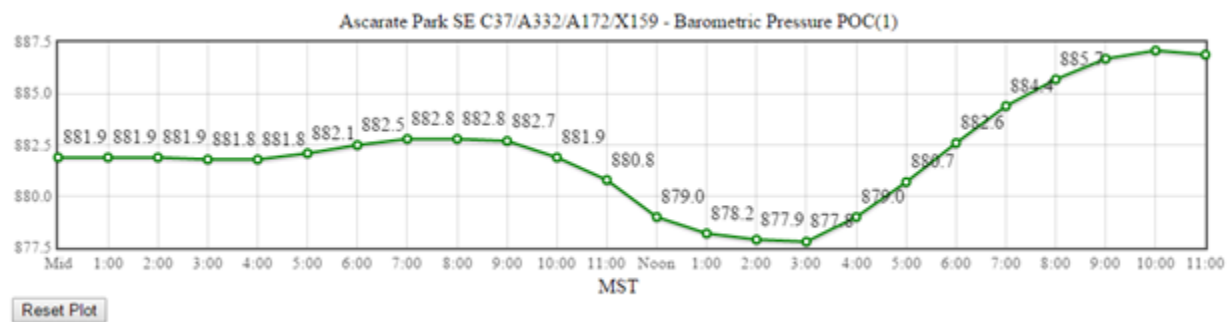
The weather parameters taken from the Azcarate monitoring station shows a sustain wind gust of 50 miles per hour during a period of 5 hours during the event. Meanwhile, the temperature reported a drop from 76F to 55F on all parts of the event, and was correlated with the visibility which had a drop to almost 0 during the middle of the event. Another fact was that both pressure and humidity remained low during the start and middle of the event, with a little increase during the final phase of the event.

As observed on the stations the PM10 started to rise at 1pm to 2145 microgram per cubic meter, then it peaked at 2pm at 4687 and 4526 microgram per cubic meter at 3pm. Later, it went down to the 1000's microgram per cubic meter between 4pm and 6pm.

The PM<sub>2.5</sub> started to rise to 324 microgram per cubic meter at 1pm, reaching a peak of 719 and 603 microgram per cubic meter at 2pm and 3pm respectively. Later it went down to the 100's microgram per cubic meter on the ongoing hours of the event.

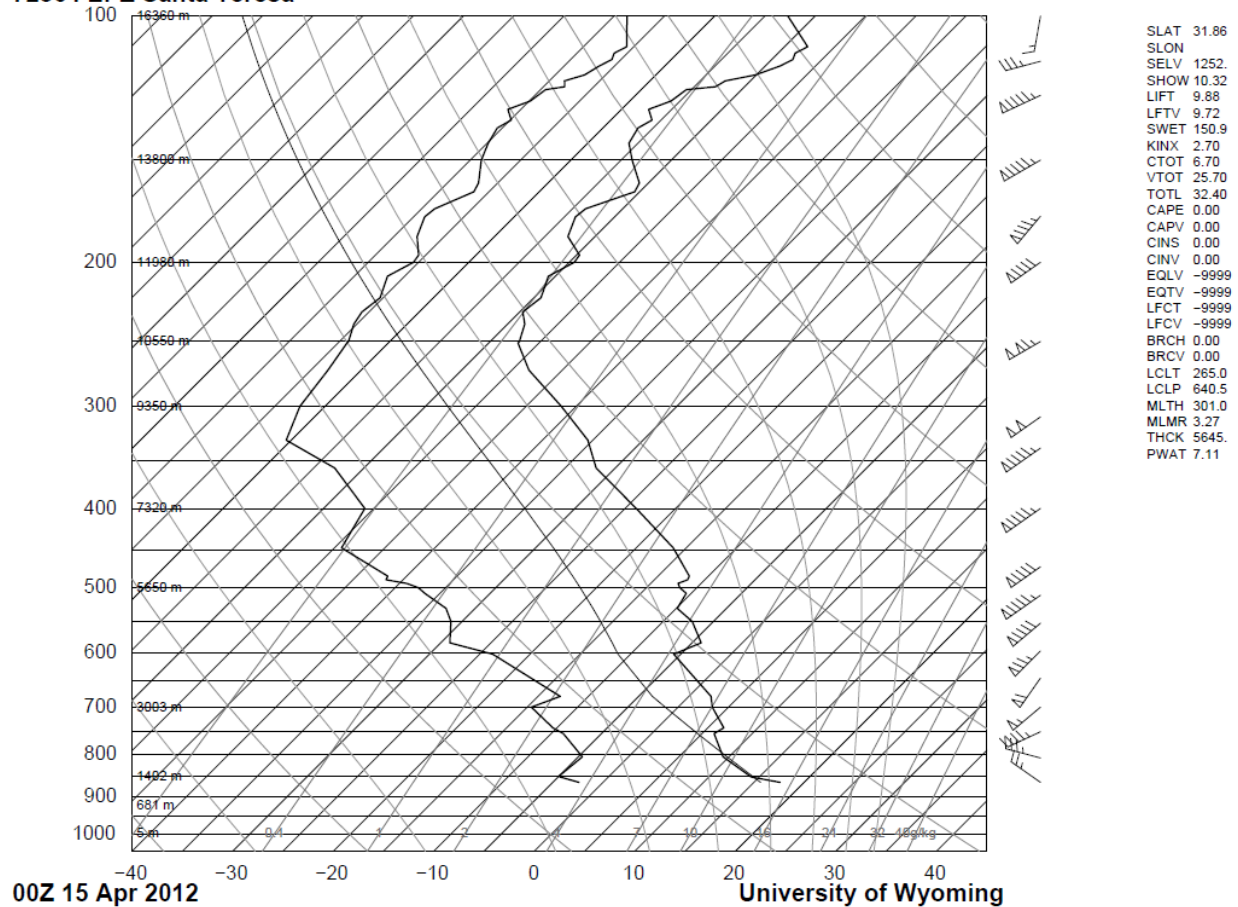






Graph 11. Weather conditions at Azcarate Monitoring station

# 72364 EPZ Santa Teresa



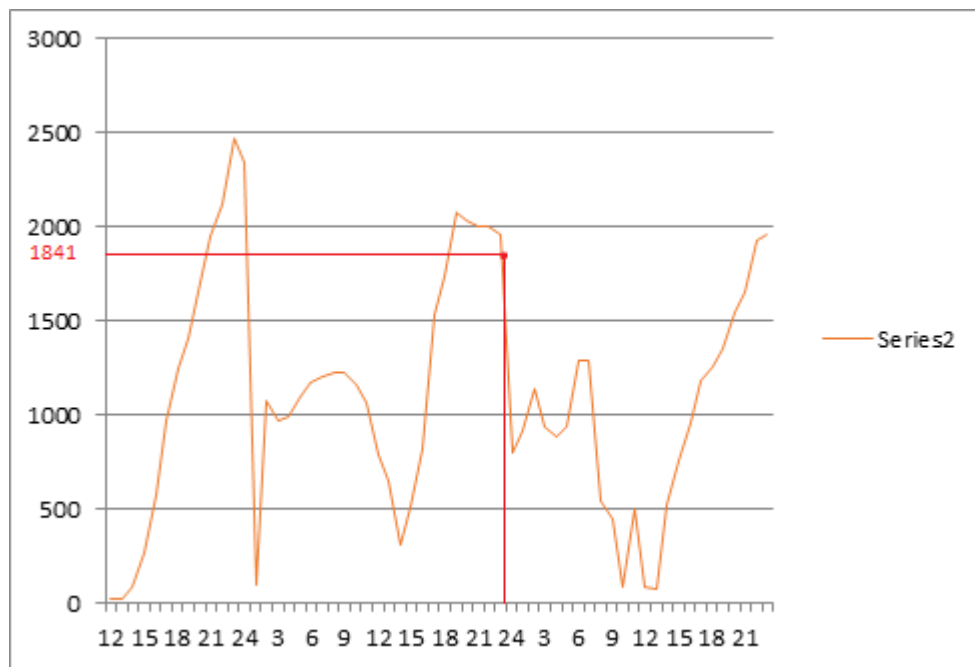
Graph 12. Sounding chart from the University of Wyoming

April 14, 2012, shows 1841 meters above ground slight inversion at top.

The Fluctuations in the PBL during the storm and the thermal convective currents in the pbl responsible for mixing the dust to the higher elevations.

The fact that the PBL often did not drop down to near the surface at dark following these dust storms is due to the moderate to strong west to northwest winds following these strong synoptic events (upper trough and surface cold fronts) which kept the lower winds up (mixing) and the

PBL elevated as well until about 10-12z when the winds died off and radiation cooling set in with a correspondingly lower PBL often at the top of the surface inversion at sunrise.



Graph 13. WRF PBLH result for April 14, 2012

The PBLH extract from WRF shown above, the inversion is at 1841 meters AGL, which Started on April 13 2012 12Z (Zulu time) and ended on April 15 2012 00Z.

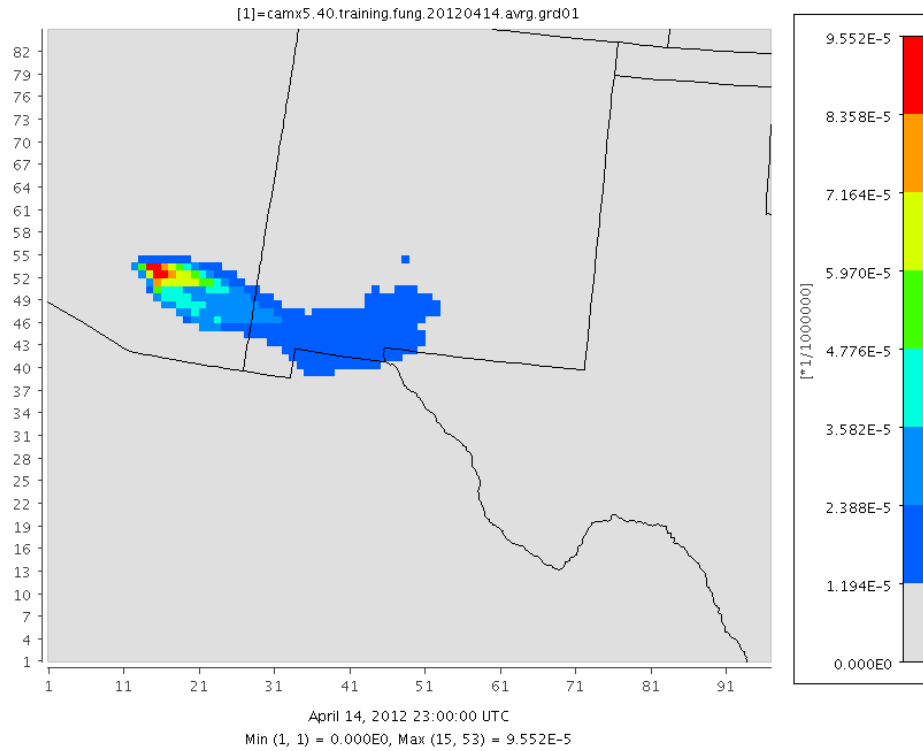


Figure 23. Contour plot of PM 10

The point source created by EPS3 is located between the Phoenix and Tucson area; this input is to simulate the dust with characteristics of PM2.5 and PM10 with values of 15000 metric tons per year and 64000 metric tons per year respectively (2011 Periodic Emission Inventory for PM10 for the Maricopa County, Arizona PM10 Nonattainment Area). By using WRF, the weather conditions were simulated to obtain an input for CMAQ.

The simulation from CAMx for PM10 at 2300 UTC, shows the dust plume originated on Arizona landing in El Paso Area for April 14, 2012 at 23:00 UTC or 4:00pm MST.

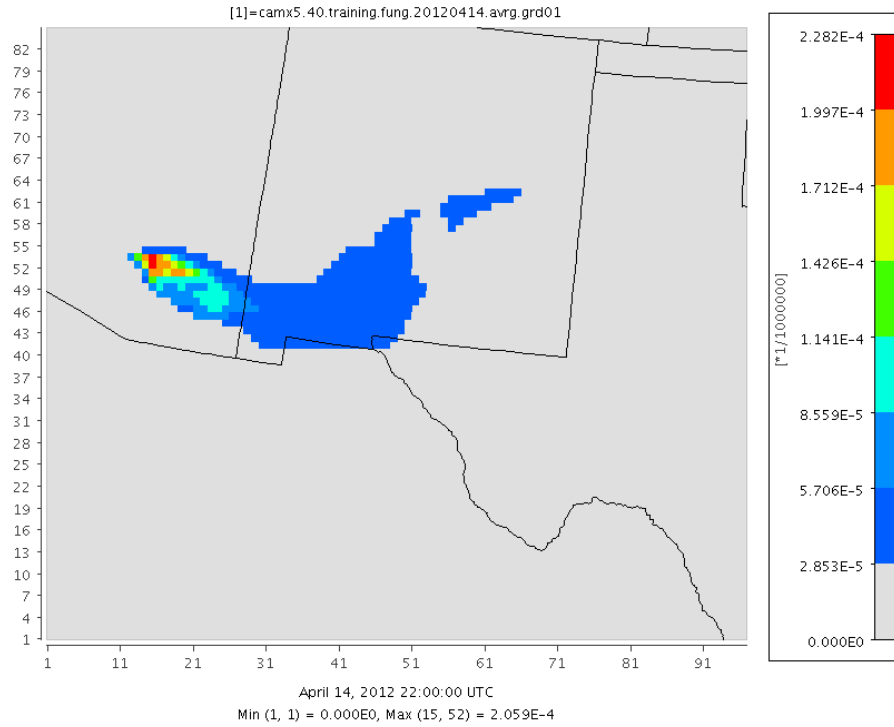


Figure 24. Contour plot of PM 2.5

The simulation from CAMx for PM2.50 at 2200 UTC, shows the dust plume originated on Arizona landing in El Paso Area, for April 14, 2012 at 22:00 UTC or 3:00pm MST.

## Chapter 4

### Conclusion

For the first project, the simulated ozone using CB4 and CB5 were correlated against each other. The results showed a common problem with air quality models, simulations display less variability in modeled ozone than in comparison with experimental data from measured data. Air quality models underestimate the response of ozone to emissions and meteorological changes, one aspect could be that ozone measurements are made into a single point source, rather than the simulation that is in a complete grid. Other possibility is that mixing layer could impact nitric oxide emissions. Another possibility is that the bias on the development and testing of air quality models, where are evaluated against environmental chamber data, where the chemistry process occurs at high concentrations, leading to a bias on high ozone concentrations against lower mixing ratios of ozone concentrations.

For the second project, model simulations with the 2030 baseline emissions predict higher peak ozone in the western and central area compared to the 2008 baseline, with reduction of NO<sub>x</sub> to 50% ozone levels are predicted to be lowered to 15% in all areas except the western and central areas, therefore reductions of NO<sub>x</sub> of 90% will be necessary to obtain the standard. The NO<sub>x</sub> focused strategy is based with sufficient NO<sub>x</sub> reduction, ozone formation will transition from VOC to NO<sub>x</sub> limited ozone formation. The response of ozone to reduction of VOC are beneficial but becomes less effective as the NO<sub>x</sub> concentrations are reduced to low levels, this means that NO<sub>x</sub> focused strategy in reductions exceeding 80% from 2008 levels will be required to attain ozone levels on the western and central basin.

For the third project, experimental data from satellites and monitoring stations showed a dust storm event on April 12, 2012. By correlating with Hysplit and Windrose the source of the event took place in the Phoenix-Tucson area and approaching El Paso between 2 and 3 pm MST. By using WRF, the meteorological conditions were able to be reproduced almost identically and the source dust (PM<sub>2.5</sub> and PM<sub>10</sub>) created with EPS3 was transported in a same way as the event. CAMx simulations were able to show the same patterns for the dust as the satellite images. Another observed behavior was the PBLH were normally drops to zero at 24 UTC, but during the event it maintained its height.

In summary, open source software, such as CMAQ, CAMx and WRF provide flexibility and support for parallel process optimization. The three projects used those air quality models and were modified and enhanced to run in parallel in a high performance cluster. Therefore, air quality models take full advantage of processing and time by running in a parallel environment. The models have been successfully applied in three different scenarios to improve on their air quality forecasting capabilities.



## References

2011 Periodic Emission Inventory for PM<sub>10</sub> for the Maricopa County, Arizona PM<sub>10</sub> Nonattainment Area, January 2014

Amit Jain, Beowulf Cluster Design and Setup

Boise State University, April 26, 2006

Abhishek Gupta, Cluster Schedulers, Department of Computer Science and Engineering Indian Institute Of Technology Guwahati

Arteta, J., Cautenet, S., Taghavi, M., N. Audiffren, Impact of two chemistry mechanisms fully coupled with mesoscale model on the atmospheric pollutants distribution. *Atmos. Environ.* 40, 7983–8001, 2006.

Byun, D., and K. L. Schere, Review of the governing equations, computational algorithms, and other components of the Models-3 Community Multiscale Air Quality (CMAQ) modeling system. *Applied Mechanics Reviews* 59, 51–77, 2006.

Bhave, P. V., G. A. Pouliot, and M. Zheng, 2007. Diagnostic model evaluation for carbonaceous PM<sub>2.5</sub> using organic markers measured in the southeastern U.S., *Environ. Sci. Technol.*, 41: 1577-1583.

Carlton, A.G., B. J. Turpin, K. Altieri, S. Seitzinger, R. Mathur, S.

Roselle, R. J. Weber, in review. CMAQ model performance enhanced when in-cloud SOA is included: comparisons of OC predictions with measurements, *Environ. Sci. Technol.*

Donohoe, Aaron S, A.Venkatram, and Battisti, David Atmospheric and surface contributions to planetary albedo 1977: Internal boundary-layer development and fumigation. In *Atmospheric Environment*, **11**, p. 479-482.

Edney, E. O., T. E. Kleindienst, M. Lewandowski, and J. H. Offenberg,  
2007. Updated SOA chemical mechanism for the Community Multi-Scale Air  
Quality model, EPA 600/X-07/025, U.S. EPA, Research Triangle Park, NC.

Faraji, M., Kimura, Y., McDonald-Buller, E., and D. Allen, Comparison of the Carbon Bond and SAPRC photochemical mechanisms under conditions relevant to southeast Texas, *Atmos. Environ.*, 42, 5821–5836, doi:10.1016/j.atmosenv.2007.07.048, 2008.

Gery, M. W., Whitten, G. Z., Killus, J. P., and Dodge, M. C.: A photochemical kinetics mechanism for urban and regional scale computer modeling, *J. Geophys. Res.*, 94(D10), 12925-12956, 1989.

Gerald L. Gipson\* Human Exposure and Atmospheric Sciences Division, National Exposure Research Laboratory, U. S. Environmental Protection Agency Research Triangle Park, NC 27711, USA

Goliff W.S., W.R. Stockwell and C.V. Lawson, The Regional Atmospheric Chemistry Mechanism Version 2, Submitted, *Atmos. Environ.*, 2012.

Gross, A. and W.R. Stockwell, Comparison of the EMEP, RADM2 and RACM Mechanisms, *J. Atmos. Chem.*, 44, 151-170, 2003.

Heo, G. and G. Yarwood, Gas-Phase Chemistry in Air Quality Models: Research Needs and Recommendations, *Environmental Manager*, September, 22-24, 2012.

Holton, James R., An Introduction to Dynamic Meteorology, Fourth Edition, p 60-65

Seinfeld, J. and S. Pandis, Atmospheric chemistry and physics: from air pollution to climate change. 2006

Jiang, W., Giroux, E., Smyth, S., Roth, H. and Yin, D. Differences Between CMAQ Fine Mode Particle and PM<sub>2.5</sub> Concentrations and their Impact on Model Performance Evaluation in the Lower Fraser Valley. 2004 Models-3 Conference. October 18–20 2004, Chapel Hill, NC

Kim, Y.; Sartelet, K.; Seigneur, C. Formation of secondary aerosols over Europe: Comparison of two gas-phase chemical mechanisms. *Atmos. Chem. Phys.* 2011, 11, 583-598.

Kuhn, M., O. J. H. Builtjes, D. Poppe, D. Simpson, W. R. Stockwell, Y. Andersson-Sköld, A. Baart, M. Das, F. Fiedler, O. Hov, F. Kirchner, P. A. Makar, J. B. Milford, M. G. M. Roemer, R. Ruhnke, A. Strand, B. Vogel, H. Vogel, Intercomparison of the gas-phase chemistry in several chemistry and transport models, *Atmos. Environ.*, 32, 693-709, 1998.

Luecken, D. J., S. Phillips, G. Sarwar, and C. Jang, Effects of using the CB05 vs. SAPRC99 vs. CB4 chemical mechanism on model predictions: Ozone and gas-phase photochemical precursor concentrations. *Atmos. Environ.*, 42, 5805–5820, 2008.

MODIS terra products, <https://ladsweb.nascom.nasa.gov/>

Russell, A. and Dennis, R.: NARSTO critical review of photochemical models and modeling, *Atmos. Environ.*, 34, 2283–2324, 2000.

Stockwell, W. R., Kirchner, F., Kuhn, M. and Seinfeld, S., A new mechanism for regional atmospheric chemistry modeling, *J. Geophys. Res.*, 102, 25847-25879, 1997.

Stockwell, W.R., C.V. Lawson, E. Saunders and W.S. Goliff, A Review of Tropospheric Atmospheric Chemistry and Gas-Phase Chemical Mechanisms for Air Quality Modeling, Atmosphere, 3, 1-32, 2012. doi:10.3390/atmos30100012011

V. S. Sunderam , PVM: A Framework for Parallel Distributed Computing, Concurrency: Practice and Experience, 2, 4, pp 315--339, December, 1990

W. Gropp, E. Lusk, and A. Skjellum, Using MPI: Portable Parallel Programming with the Message-Passing Interface, MIT Press, 1999.

Yarwood, G., Rao, S., Yocke, M., and G. Z. Whitten, Updates to the Carbon Bond chemical mechanism: CB05, Final Report to the US EPA, RT-0400675, 8 December 2005, [http://www.camx.com/publ/pdfs/CB05 Final Report 120805.pdf](http://www.camx.com/publ/pdfs/CB05%20Final%20Report%20120805.pdf), 2005.

## Curriculum Vitae

Roberto Alfonso Perea Martinez was born on November 17, 1977 in Mexico City. The first son of Roberto Perea, M.D. and Virginia Martinez M.D. both graduated from medical school with specialist degree. He graduated from High school in 1996 in Chihuahua City, after that he enrolled in the University of Texas at El Paso to pursue a degree in Electrical engineering. In May of 2002, he received his bachelor degree in electrical engineering. In the fall of 2002 he entered graduate school at The University of Texas at El Paso. While in the Electrical and computer engineer department, he worked as a system administrator for the UNIX computer laboratory. On 2004, he received his Master degree on electrical and computer engineering and continued a full time job at the information technology department at the University of Texas at El Paso. In fall of 2009, he enrolled in the Environmental Science program to pursue a PhD.

Permanent address: 6201 Escondido St. 4H

El Paso, Texas 79912

This Dissertation was typed by Roberto Perea